

# FAST LINK ADAPTATION TECHNIQUE FOR TIME VARYING MULTIPATH CHANNELS

## A DISSERTATION

*Submitted in partial fulfillment of the  
requirements for the award of the degree*

*of*

MASTER OF TECHNOLOGY

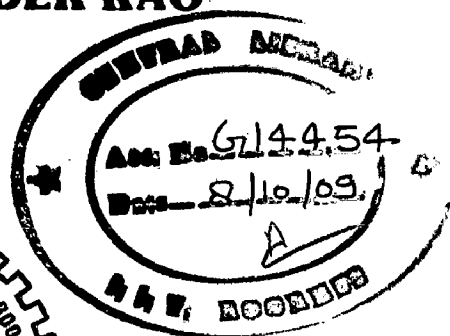
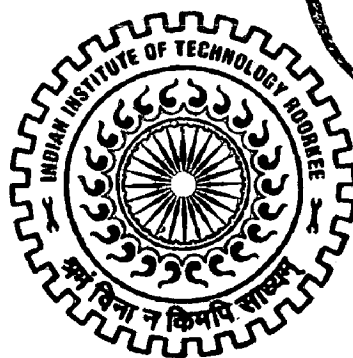
*in*

ELECTRONICS AND COMMUNICATION ENGINEERING

(With Specialization in Communication Systems)

*By*

**B.SATEESH CHANDER RAO**



DEPARTMENT OF ELECTRONICS AND COMPUTER ENGINEERING  
INDIAN INSTITUTE OF TECHNOLOGY ROORKEE  
ROORKEE - 247 667 (INDIA)

JUNE, 2009

## CANDIDATE'S DECLARATION

---

I hereby declare that the work, which is presented in this dissertation report entitled, "FAST LINK ADAPTATION TECHNIQUE FOR TIME VARYING MULTIPATH CHANNELS" towards the partial fulfillment of the requirements for the award of the degree of **Master of Technology** with specialization in **Communication Systems**, submitted in the Department of Electronics and Computer Engineering, Indian Institute of Technology Roorkee, Roorkee (India) is an authentic record of my own work carried out during the period from June 2008 to June 2009, under the guidance of **Dr. S. K. VARMA**, Professor, Department of Electronics and Computer Engineering, Indian Institute of Technology Roorkee.

I have not submitted the matter embodied in this dissertation for the award of any other Degree or Diploma.

Date: 29/6/2009

Place: Roorkee

  
**B. SATEESH CHANDER RAO**


---

## CERTIFICATE

This is to certify that the above statement made by the candidate is correct to the best of my knowledge and belief.

Date: 29/6/2009

Place: Roorkee

  
**Dr. S. K. VARMA,**  
Professor, E&CE Department,  
IIT Roorkee,  
Roorkee – 247 667 (India).

# ACKNOWLEDGMENTS

---

I would like to extend my heartfelt gratitude to my guide, **Dr. S. K. VARMA** for his able guidance, valuable suggestions and constant attention. It is his constant encouragement that inspired me throughout my dissertation work. I consider myself fortunate to have my dissertation done under him.

I am indebted to all my teachers who shaped and molded me. I would like to express my deep sense of gratitude to all the authorities of Department of Electronics and Computer Engineering, IIT Roorkee for providing me with the valuable opportunity to carry out this work and also providing me with the best of facilities for the completion of this work.

I am very thankful to the staff of Signal Processing Lab for their constant cooperation and assistance.

I am indebted to my parents for everything that they have done for me. They always supported me with their love, care and valuable advices. Thanks are also due to all my classmates who have helped me directly or indirectly in my work.

Last, but not the least my deepest gratitude to the Almighty God whose Divine grace provided me guidance, strength and support always.

**B .SATEESH CHANDER RAO**

# ABSTRACT

---

Multicarrier communication systems with adaptive modulation and coding systems such as OFDM are well suited for high speed and mobility oriented networks like mobile WiMAX, that has to support users in different fading and mobility conditions. It is also important in practical wireless systems for improving the accuracy of the link adaptation and the efficiency of radio-resource-management. Bit Error Rate (BER) prediction over fast varying channel has emerged as an active research area.

Exponential Effective SINR Mapping (EESM) is a mapping scheme that facilitates system level simulations by accounting the system performance in multi state channel in terms of an Additive White Gaussian Noise (AWGN) Channel. The method comprises of the steps of providing individual channel quality values for the different channels and determining a quality measure indicative of the link quality by averaging the individual channel quality values in exponential domain. The BER of the system in that multi state channel thus gives an insight of the modulation and coding schemes to be used for the given link. The simulation results are discussed for different channel realizations, different modulation and coding schemes.

This method can be extended to handle more advanced link enhancement such as Alamouti coding and the resulting scheme would be Alamouti based EESM scheme.

# CONTENTS

---

<b>CANDIDATE’S DECLARATION .....</b>	<b>i</b>
<b>ACKNOWLEDGEMENTS.....</b>	<b>ii</b>
<b>ABSTRACT.....</b>	<b>iii</b>
<b>TABLE OF CONTENTS.....</b>	<b>iv</b>
<b>LIST OF FIGURES.....</b>	<b>vi</b>
<b>LIST OF TABLES.....</b>	<b>vii</b>
<b>LIST OF ACRONYMS.....</b>	<b>viii</b>
<b>CHAPTER 1: INTRODUCTION .....</b>	<b>1</b>
1.1 Problem Statement.....	5
1.2 Organization of the Report .....	5
<b>CHAPTER 2: ORTHOGONAL FREQUENCY DIVISION MULTIPLEXING</b>	
.....	<b>6</b>
2.1 Multicarrier Modulation .....	6
2.2 OFDM .....	8
2.2.1 Block Transmission with Guard Intervals.....	9
2.2.2 Circular Convolution and the DFT.....	10
2.2.3 The Cyclic Prefix.....	11
2.2.4 Frequency Equalization.....	13
2.2.5 An OFDM Block Diagram.....	14
<b>CHAPTER 3: MIMO AND CODING</b>	
.....	<b>15</b>
3.1 Classical Maximal-Ratio Receive Combining (MRCC) Scheme .....	15
3.2 Alamouti Transmit Diversity Schemes.....	17
3.3 Assumptions.....	21
3.4 Convolutional Coding.....	21

<b>CHAPTER 4: LINK ADAPTATION FOR TIME VARYING MULTIPATH CHANNELS.....</b>	<b>23</b>
4.1 Slow and Fast Link Adaptation.....	23
4.2 Channel Modeling .....	23
4.3 Derivation of the basic Exponential ESM.....	25
4.4 A Generalized Exponential ESM.....	28
4.5 Link Abstraction.....	28
4.6 Calibration of $\beta$ .....	29
<b>CHAPTER 5: SIMULATION RESULTS .....</b>	<b>32</b>
5.1 Simulation of STCs and EESM Scheme.....	32
5.2 Flow chart for implementing Space Time Codes.....	34
5.3 Flowchart for OFDM.....	35
5.4 Flow Chart used for Simulation of EESM Scheme.....	36
5.4 Results of Simulations.....	37
<b>CHAPTER 6: CONCLUSION.....</b>	<b>40</b>
<b>REFERENCES.....</b>	<b>41</b>

# LIST OF FIGURES

---

Figure No.	Figure Name	Page No.
1.1	Forecast of Broadband users (World wide).....	2
2.1	Basic Multicarrier Transmitter.....	7
2.2	Basic Multicarrier Receiver.....	8
2.3	Effect of Multicarrier Modulation in a Frequency Selective Channel.....	9
2.4	The OFDM Cyclic Prefix.....	11
2.5	Circular Convolution created by OFDM Cyclic Prefix.....	13
2.6	An OFDM System in Vector notation.....	14
3.1	Classical MRRC Scheme.....	15
3.2	Alamouti two by one Transmit Diversity Scheme.....	17
3.3	Feed Forward Convolutional Encoder (Memory Length 2, Rate .5).....	22
4.1	Block Diagram for Transmitter (above) and Receiver (below) Blocks using OFDM.....	29
4.2	Method of EESM showing instantaneous SINR Mapping to BLER.....	30
5.1	Flow Chart for implementing Space Time Codes.....	34
5.2	Flow Chart for implementing OFDM system .....	35
5.3	Flow Chart used for Simulation of EESM Scheme.....	36
5.4	BER vs SNR in incorporating Diversity to the Transmission .....	37
5.5	EESM Abstraction 4QAM Rate .5 Beta 1.6.....	37
5.6	EESM Abstraction 4QAM Rate .75 Beta1.7.....	38
5.7	EESM Abstraction 16QAM Rate .5 Beta 5.5.....	38
5.8	EESM Abstraction 64QAM Rate .5 Beta17.3.....	39

# LIST OF TABLES

---

<b>Table No.</b>	<b>Table Name</b>	<b>Page No.</b>
3.1	Symbol representation of Antennas with time.....	18
3.2	Definition of Channels between Transmitter and Receiver.....	19
3.3	Notation for received signals and Transmit Antennas.....	19
5.1	Delay and Power value for Ped A and Ped B Channel Models.....	33



# LIST OF ACRONYMS

---

AWGN	Additive White Gaussian Noise
BER	Bit Error Rate
BLER	Block Error Rate
BPSK	Binary Phase Shift Keying
BS	Base Station
CDF	Cumulative Distribution Function
CP	Cyclic Prefix
CSI	Carrier State Information
DL	Down Link
EESM	Effective Exponential SINR Mapping
FEC	Forward Error Correcting
ICI	Inter Channel Interference
IID	Independently and Identically Distributed
ISI	Inter Symbol Interference
LA	Link Adaptation
MCS	Modulation Coding Scheme
MIMO	Multiple Input Multiple Output
MISO	Multiple Input Single Output
ML	Maximum Likelihood
OFDM	Orthogonal Frequency Division Multiplexing
PDF	Probability Distribution Function
PDP	Power Delay Profile
PED A	Pedestrian A
QAM	Quadrature Amplitude Modulation
QoS	Quality of Service
QPSK	Quadrature Phase Shift Keying

# Chapter 1

## Introduction

---

Broadband wireless sits at the confluence of two of the most remarkable growth stories of the telecommunications industry in recent years. Both wireless and broadband have on their own enjoyed rapid mass-market adoption [1]. During the same period, the internet grew from being a curious academic tool to having about a billion users. This incredible growth of the Internet is driving demand for higher-speed internet-access services, leading to a parallel growth in broadband adoption. In less than a decade, broadband subscription worldwide has grown from few millions to over 300 million [2].

A review the state of fixed broadband wired access today is discussed as a part of this aspect. Digital Subscriber Line (DSL) technology, which delivers broadband over twisted-pair telephone wires, and cable modem technology, which delivers over coaxial cable TV plant, are dominant mass-market broadband access technologies until today. Both of these technologies typically provide up to a few megabits per second of data to each user, and continuing advances are making several tens of megabits per second possible. Since their initial deployment in the late 1990s, these services have enjoyed considerable growth. Today the number of broad band subscribers is more than 300 million, and is projected to grow to over 800 million by 2012 [3]. The availability of a wireless solution for broadband could potentially accelerate this growth.

The following are some common applications of broadband access in present days. Broadband users worldwide are finding that it dramatically changes how we share information, conduct business, and seek entertainment. Broadband access not only provides faster web surfing and quicker file downloads but also enables several multimedia applications, such as real-time audio and video streaming, multimedia conferencing, and interactive gaming. Broadband connections are also being used for voice telephony using Voice-Over-Internet Protocol (VoIP) technology. More advanced broadband access systems, such as Fiber-to-the-Home (FTTH) and Very High Data Rate Digital Subscriber Loop (VDSL), enable such applications as entertainment-quality video, including High-Definition TV (HDTV) and Video on

Demand (VoD). As the broadband market continues to grow, several new applications are likely to emerge in the future. .

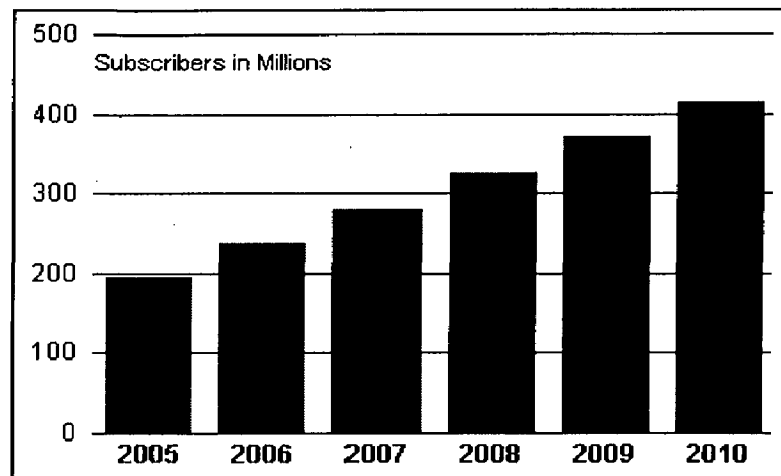


Figure 1.1 Forecast of Broadband users (World wide) [3]

The history of broadband wireless as it relates to WiMAX [4] reveals that it can be a competitive alternative to traditional wireline-access technologies. Spurred by the deregulation of the telecom industry and the rapid growth of the Internet, several competitive businessmen were motivated to find a wireless solution to bypass current wireline service providers. During the past decade, a number of wireless access systems have been developed, mostly by start-up companies motivated by the disruptive potential of wireless. These systems varied widely in their performance capabilities, protocols, frequency spectrum used, applications supported, etc. Some systems were commercially deployed only to be decommissioned later. Successful deployments have so far been limited to a few niche applications and markets.

IEEE 802.16 is mainly aimed at providing Broadband Wireless Access (BWA) and thus it may be considered as an attractive alternative solution to wired broadband technologies like DSL and cable modem access [4]. Its main advantage is fast deployment which results in cost savings. Such installation can be beneficial in very crowded geographical areas like cities and in rural areas where there is no wired infrastructure. The IEEE 802.16 standard provides network access to buildings through external antennas connected to radio base stations. The frequency band supported by the standard covers 2 to 66 GHz. In theory, the IEEE 802.16 standard, known also as WiMAX, is capable of covering a range of 50 km with a bit rate of 75 Mb/s. However, in the real world, the rate obtained from WiMAX is about 12 Mb/s

with a range of 20 km. The Intel WiMAX solution for fixed access operates in the licensed 2.5 GHz and 3.5 GHz bands and the license-exempt 5.8 GHz band. A brief history of the standard is presented here:

Research for a new standard of Wireless MAN dates to early 1998. In 2001 the 802.16 standard was finally approved by the IEEE.

*IEEE 802.16-2001:* IEEE 802.16 was formally approved by the IEEE in 2001. It is worth mentioning that many basic ideas of 802.16 were based on the Data Over Cable Service Interface Specification (DOCSIS). This is mainly due to the similarities between the Hybrid Fiber-Coaxial (HFC) cable environment and the broadband wireless access environment. 802.16 utilizes the 10 to 66 GHz frequency spectrum and thus is suitable for Line-of-Sight (LOS) applications. With its short waves, the standard is not useful for residential settings because of the Non-Line-of-Sight (NLOS) characteristics caused by rooftops and trees.

*IEEE 802.16a-2003:* This extension of the 802.16 standard covers fixed BWA in the licensed and unlicensed spectrum from 2 to 11 GHz. The entire standard along with the updated amendments was published on April 1, 2003. This amendment was mainly developed for NLOS applications and thus it is a practical solution for the last-mile problem of transmission where obstacles like trees and buildings are present. IEEE 802.16a supports PMP network topology and optional mesh topology BWA. It specifies three air interfaces: single-carrier modulation, 256-point transform Orthogonal Frequency Division Multiplexing (OFDM), and 2048-point transform Orthogonal Frequency Division Multiple Access (OFDMA). The IEEE 802.16a standard specifies channel sizes ranging from 1.75 to 20 MHz. This protocol supports low latency applications such as voice and video.

*IEEE 802.16-2004:* This standard revises and consolidates 802.16-2001, 802.16a-2003, and 802.16c-2002. WiMAX technology based on the 802.16-2004 standards is rapidly proving itself as a technology that will play a key role in fixed broadband Wireless MANs. The MAC layer supports mainly PMP architecture and mesh topology as an option. The standard is specified to support fixed wireless networks. The mobile version of 802.16 is known as mobile WiMAX or 802.16e.

*IEEE 802.16e (mobile WiMAX):* This is the mobile version of the 802.16 standard. This amendment aims at maintaining mobile clients connected to a MAN while

moving around. It supports portable devices from mobile smart-phones and Personal Digital Assistants (PDAs) to notebook and laptop computers. IEEE 802.16e works in the 2.3 GHz and 2.5 GHz frequency bands.

In addition to the IEEE 802.16 working group, companies in the industry also have formed the WiMAX forum to promote the development and deployment of WiMAX systems [5]. Several vendors recently released the first mobile products certified by the WiMAX forum industry group. In a recent study, the WiMAX forum projected more than 93 million mobile WiMAX users globally by 2012.

The technology faces fierce competition in the wireless market [3]. Existing third-generation (3G) cellular technologies—Code Division Multiple Access 2000 (CDMA2000) and the Universal Mobile Telecommunications System (UMTS) are already available and supply some of mobile WiMAX's functionality, although not its combination of high data rates and long transmission ranges. The size of devices employed by 3G are bulky and consume more power whereas it is the other way round with small and rugged devices consuming less power. However fixed WiMAX has dominant capabilities than 3G, the mobile version capacities are yet to be proved. In addition to competing technologies seen above, UMTS's 4G version, Long Term Evolution (LTE), have burst speeds close to mobile WiMAX's rates and will be fully TCP/IP-based. LTE will thus be able to provide television, telephony, and internet services. However, proponents did not plan to release the technology commercially until 2011 or 2012.

WiMAX has already been deployed in countries such as India, Indonesia, Japan, Korea etc. There are experimental implementations in France, Spain, and the UK. Widespread global deployment is planned for the next couple of years [6].

Intel has announced plans to incorporate mobile WiMAX capabilities into its next-generation Centrino2 laptop Wi-Fi chips, slated to start shipping in the near future. Nokia plans to incorporate this chip family in its next-generation N810 Internet tablet computer.

WiMAX (IEEE 802.16) being introduced as one of the major future key technologies for wireless broadband, performance modeling and simulations are required to obtain the best result from being deployed. In WiMAX, the channel is divided into

thousands of orthogonal subcarriers resulting is what is called OFDM [4]. One of the major challenges in modeling WiMAX is to evaluate the channel quality and model the combined effect of interference on these subcarriers. EESM is a commonly employed method to combine Signal to Interference and Noise Ratios (SINR) in such multi-carrier environments. EESM requires the use of a 'beta' parameter that needs to be set correctly so that the channel model results in accurate BLER for a given modulation and coding scheme. In this thesis a simulation model of the WiMAX physical layer is implemented and simulations are carried out to determine the beta values for a number of modulating and coding schemes used in WiMAX networks.

## **1.1 Problem Statement**

This work is aimed at implementing an Effective SINR Mapping method for OFDM systems in Frequency Selective Fading channels, which maps Block Error Rate (BLER) from Frequency Selective Channel to an AWGN Channel.

The work is presented as follows:

- Study of OFDM systems, Exponential Effective SINR Mapping Scheme, MIMO, Modulation and Coding Schemes.
- Implementing EESM scheme in evaluating performances of different MCSs over Frequency Selective Channels.

## **1.2 Organization of the Report**

Chapter 1 gives an overview of the evolution of the wireless systems, a brief description about 4G systems. It summarizes the problem statement for this thesis work.

Chapter 2 describes the basic ideas of OFDM systems.

Chapter 3 mainly discusses about Multiple Antenna Schemes, Channel Coding Techniques.

Chapter 4 discusses about the EESM technique, which relates System level Simulation and that of Link Level Simulation.

Chapter 5 presents the simulation results.

In chapter 6 conclusion of this dissertation is given.

## Chapter 2

# Orthogonal Frequency Division Multiplexing

---

Orthogonal Frequency Division Multiplexing (OFDM) is a multicarrier modulation technique that has recently found wide adoption in a widespread variety of high-data-rate communication systems. These include digital subscriber lines, wireless LANs (802.11a/g/n), Digital Video Broadcasting (DVB), and now WiMAX and other emerging wireless broadband systems such as the proprietary Flash-OFDM developed by Flarion (now QUALCOMM), and 3G LTE and fourth generation cellular systems [4]. OFDM's popularity for high-data-rate applications stems primarily from its efficient and flexible management of Inter Symbol Interference (ISI) in highly dispersive channels.

As channel delay spread  $\tau$  becomes an increasingly large multiple of the symbol time  $T_s$ , the ISI becomes very severe. By definition, a high-data-rate system will generally have  $\tau \gg T_s$ , since the number of symbols sent per second is high [7]. In a non line of sight system, such as WiMAX, which must transmit over moderate to long distances, the delay spread will also frequently be large. In short, wireless broadband systems of all types will suffer from severe ISI and hence will require transmitter and/or receiver techniques that overcome the ISI.

### 2.1 Multicarrier Modulation

The basic idea of multicarrier modulation is quite simple and follows naturally from the competing desires for high data rates and ISI-free channels. In order to have a channel that does not have ISI, the symbol time  $T_s$  has to be larger, often significantly larger than the channel delay spread  $\tau$ . Digital communication systems simply cannot function properly if ISI is present. An error floor quickly develops, and as  $T_s$  approaches or falls below  $\tau$ .

Multicarrier modulation divides the wideband incoming data stream into  $L$  narrowband substreams, each of which is then transmitted over a different orthogonal-frequency subchannel. The number of sub streams  $L$  is chosen to make the symbol time to make the substream bandwidth less than the channel-coherence bandwidth. This ensures that the substreams will not experience significant ISI.

The illustration of a multicarrier transmitter and receiver is given in Fig 2.1 and Fig 2.2 (figure in next page). Essentially, a high data rate signal of rate  $R$  bps and with a pass band bandwidth  $B$  is broken into  $L$  parallel substreams, each with rate  $R/L$  and pass band bandwidth  $B/L$ . After passing through the channel  $H(f)$ , the received signal would appear as shown in Fig 2.3 (figure in page 9). Here it is assumed for simplicity that the pulse shaping allows a perfect spectral shaping so that there is no subcarrier overlap. As long as the number of subcarriers is sufficiently large to allow the subcarrier bandwidth to be much less than the coherence bandwidth, that is,  $B/L \ll B_c$ , it can be ensured that each subcarrier experiences approximately flat fading. The mutually orthogonal signals can then be individually detected, as shown in Fig 2.2 (in next page).

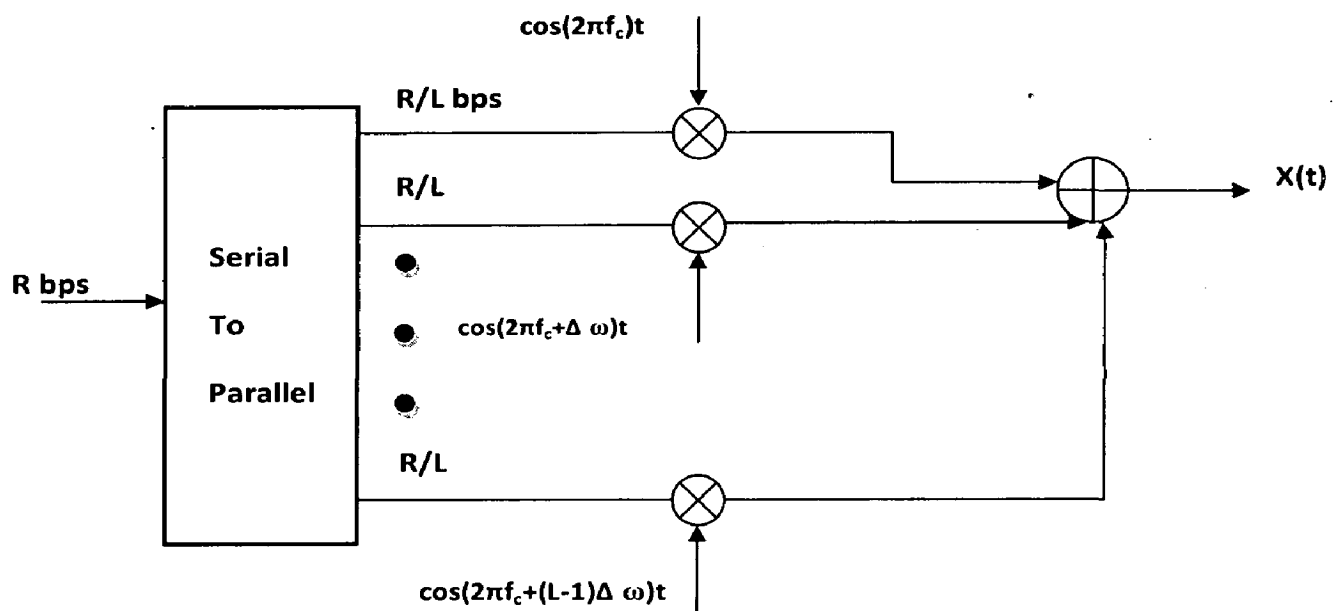


Figure 2.1 Basic multicarrier transmitter: A high-rate stream of  $R$  bps is broken into  $L$  parallel streams, each with rate  $R/L$  and then multiplied by a different carrier frequency [4]

In the time domain OFDM, the symbol duration on each subcarrier has increased to  $T = LT_s$ , so letting  $L$  grow larger ensures that the symbol duration exceeds the channel-delay spread,  $T \gg \tau$ , which is a requirement for ISI-free communication. In the frequency domain, the subcarriers have bandwidth  $B/L \ll B_c$ , which ensures flat fading, the frequency-domain equivalent to ISI-free communication.

Although this type of multicarrier modulation looks simple, it has several crucial shortcomings. First, in a realistic implementation, a large bandwidth penalty will be



inflicted, since the subcarriers can't have perfectly rectangular pulse shapes and still be time limited. Additionally, very high quality (and hence, expensive) low-pass filters will be required to maintain the orthogonality of the subcarriers at the receiver. Most important, this scheme requires  $L$  independent RF units and demodulation paths.

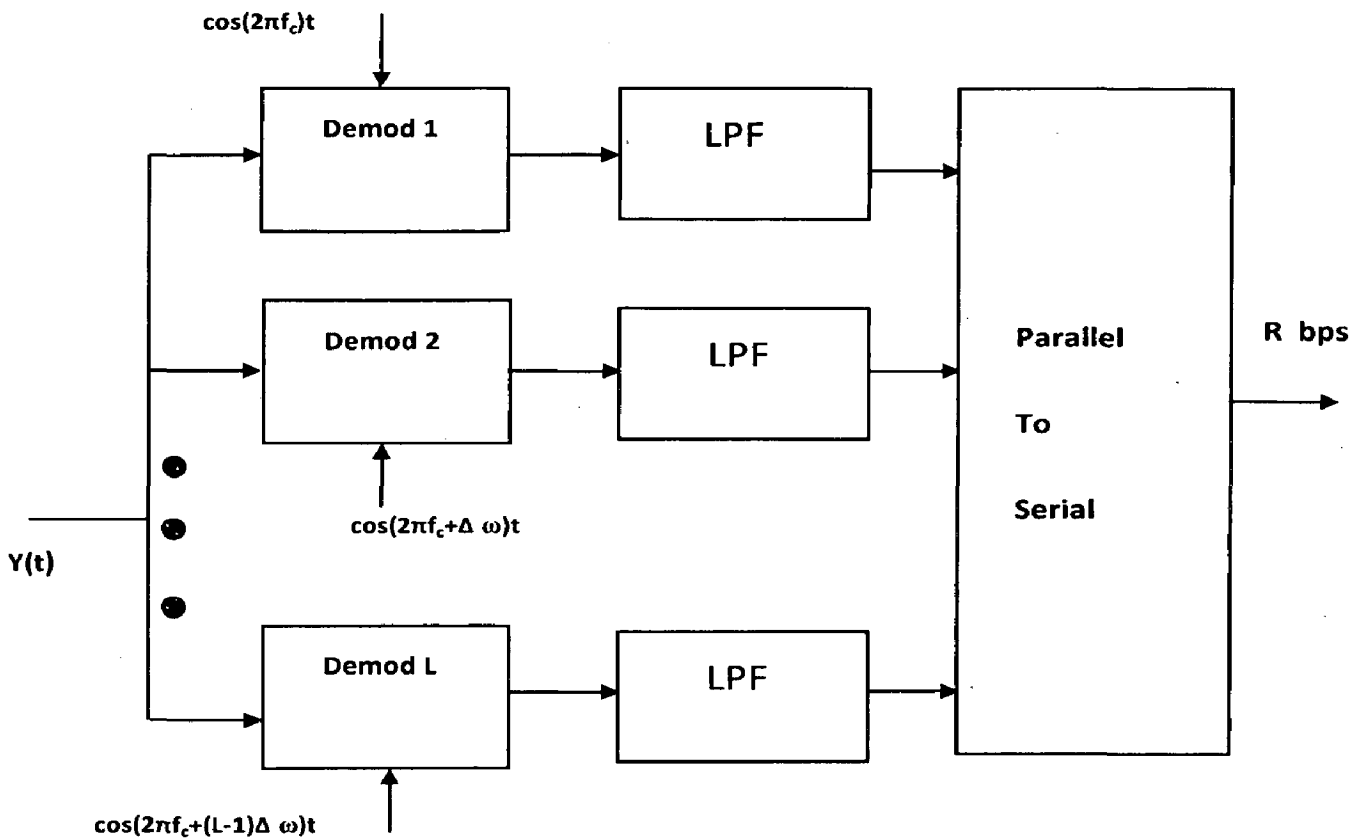


Figure 2.2 Basic multicarrier receiver: in which each subcarrier is decoded separately, requiring  $L$  independent receivers [4]

## 2.2 OFDM

In order to overcome the daunting requirement for  $L$  RF radios in both the transmitter and the receiver, OFDM uses an efficient computational technique, Discrete Fourier Transform (DFT), which lends itself to a highly efficient implementation commonly known as the Fast Fourier Transform (FFT). The FFT and its inverse, the IFFT, can create a multitude of orthogonal subcarriers using a single radio.

### 2.2.1 Block Transmission with Guard Intervals

Beginning is done by grouping  $L$  data symbols into a block known as an OFDM symbol. An OFDM symbol lasts for a duration of  $T$  seconds, where  $T=LT_s$ . In order to keep each OFDM symbol independent of the others after going through a wireless

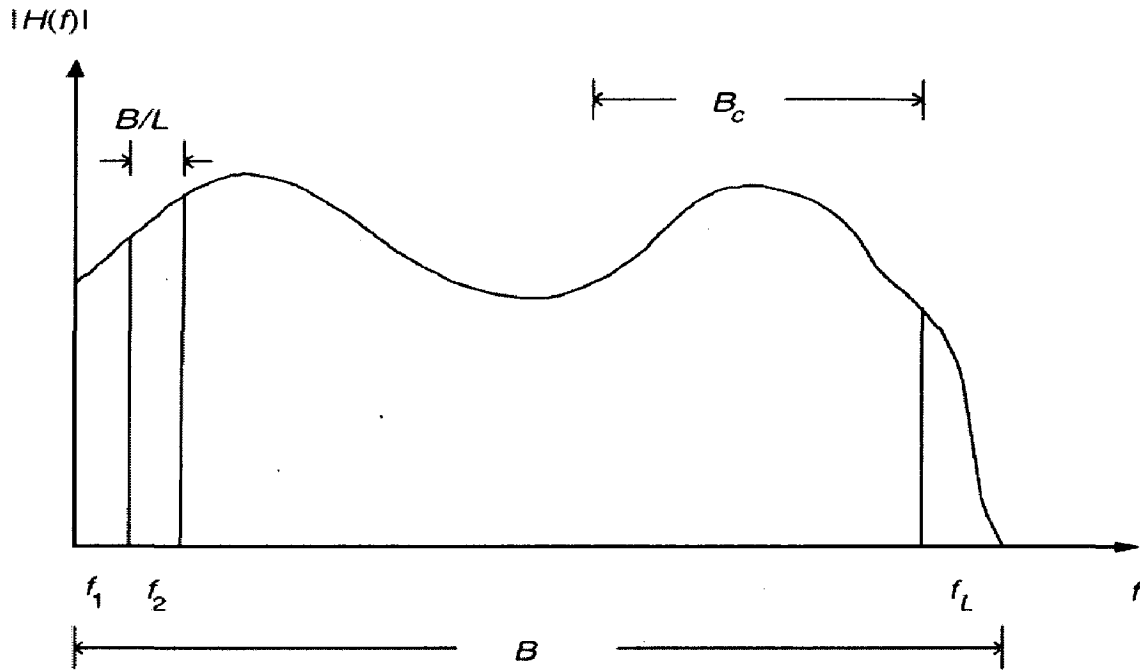
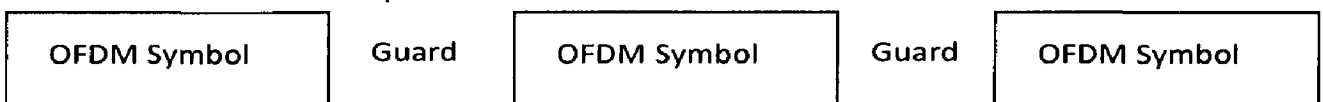
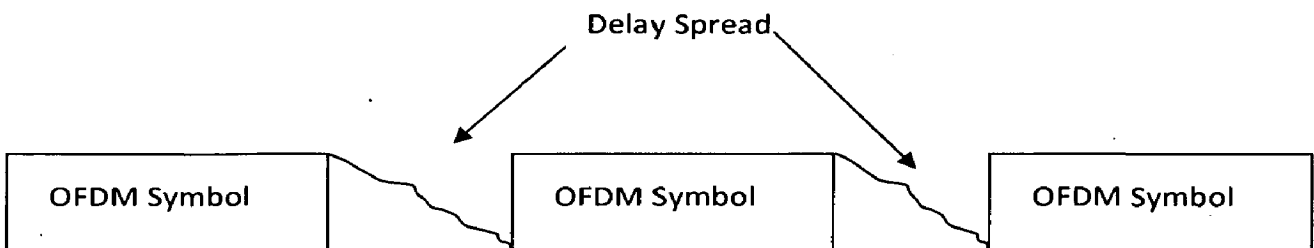


Figure 2.3 Effect of multicarrier modulation in a Frequency selective channel [4].

channel, it is necessary to introduce a guard time between OFDM symbols:



This way, after receiving a series of OFDM symbols, as long as the guard time  $T_g$  is larger than the delay spread  $\tau$  of the channel, each OFDM symbol will interfere only with itself:



OFDM transmissions allow ISI within an OFDM symbol. But by including a sufficiently large guard band, it is possible to guarantee that there is no interference between subsequent OFDM symbols.

### 2.2.2 Circular Convolution and the DFT

Now that subsequent OFDM symbols have been rendered orthogonal with a guard interval, the next task is to attempt to remove the ISI within each OFDM symbol. When an input data stream  $x[n]$  is sent through a Linear Time-Invariant (LTI), Finite Impulse Response (FIR) channel  $h[n]$ , the output is the linear convolution of the input and the channel:  $y[n]=x[n]*h[n]$ . The computing  $y[n]$  in terms of a circular convolution:

$$y[n]=x[n]\otimes h[n]=h[n]\otimes x[n] \quad (2.1)$$

where

$$x[n]\otimes h[n]=h[n]\otimes x[n] = \sum_{k=1}^{L-1} x[k]h[n - k]_L \quad (2.2)$$

and the circular function  $x[n]_L = x[n \bmod L]$  is a periodic version of  $x[n]$  with period  $L$ . In this case of circular convolution, it would then be possible to take the DFT of the channel Output  $y[n]$  to get

$$\text{DFT}\{y[n]\} = \text{DFT}\{h[n]\otimes x[n]\} \quad (2.3)$$

This yields in the frequency domain

$$Y[m] = H[m]X[m] \quad (2.4)$$

It should be noted that the duality between circular convolution in the time domain and simple multiplication in the frequency domain is a property unique to the DFT.

The  $L$  point DFT is defined as

$$\text{DFT}\{x[n]\} = X[m] = \frac{1}{\sqrt{L}} \sum_{m=0}^{L-1} x[n]e^{-j\frac{2\pi nm}{L}} \quad (2.5)$$

whereas its inverse, the IDFT, is defined as

$$\text{IDFT}\{X[m]\} = x[n] = \frac{1}{\sqrt{L}} \sum_{m=0}^{L-1} X[m]e^{j\frac{2\pi nm}{L}} \quad (2.6)$$

Referring to Eqn (2.4), this formula describes an ISI-free channel in the frequency domain, where each input symbol  $X[m]$  is scaled by a complex value  $H[m]$ . So, given knowledge of the channel-frequency response  $H[m]$  at the receiver, it is trivial to recover the input symbol by simply computing

$$\hat{X}[m] = \frac{Y[m]}{H[m]} \quad (2.7)$$

where, the estimate  $\hat{X}[m]$  will generally be imperfect, owing to additive noise, cochannel interference, imperfect channel estimation, and other imperfections. Nevertheless, in principle, the ISI, which is the most serious form of interference in a wideband channel, has been mitigated. The nature provides a linear convolution when a signal is transmitted through a linear channel.

### 2.2.3 The Cyclic Prefix

The key to making OFDM realizable in practice is the use of the FFT algorithm, which has low complexity. In order for the IFFT/FFT to create an ISI-free channel, the channel must appear to provide a circular convolution, as seen in Eqn (2.4). Adding cyclic prefix to the transmitted signal, as is shown in Fig 2.4, creates a signal that appears to be  $x[n]_L$ , and so  $y[n]=x[n]\otimes h[n]$ .

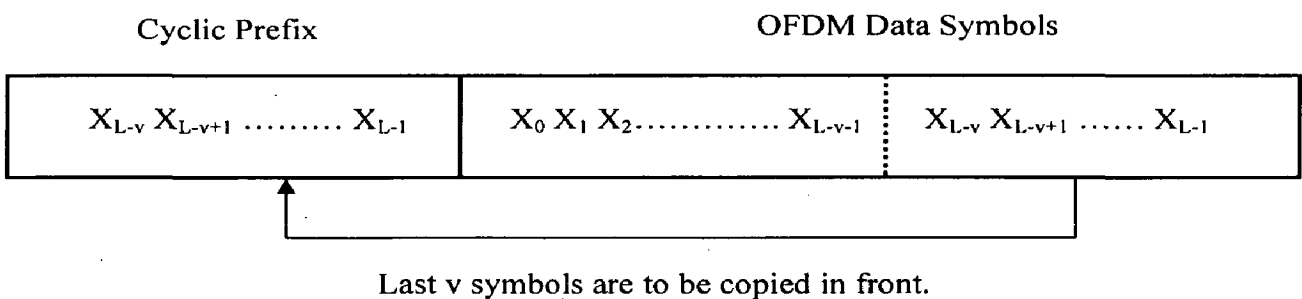


Figure 2.4 The OFDM cyclic prefix

If the maximum channel delay spread has a duration of  $v+1$  samples, adding a guard band of at least  $v$  samples between OFDM symbols makes each OFDM symbol independent of those coming before and after it, and so only a single OFDM symbol can be considered. Representing such an OFDM symbol in the time domain as a length  $L$  vector gives

$$\mathbf{X} = [x_1 \ x_2 \ x_3 \ \dots \ x_L]$$

After applying a cyclic prefix of length  $v$ , the transmitted signal is

$$\mathbf{x}_{cp} = \underbrace{[X_{L-v} X_{L-v+1} \dots X_{L-1}]}_{\text{Cyclic Prefix}} \underbrace{[X_0 X_1 \dots X_{L-1}]}_{\text{Original Data}} \quad (2.8)$$

The output of the channel is by definition  $\mathbf{y}_{cp} = \mathbf{h} \otimes \mathbf{x}_{cp}$ , where  $\mathbf{h}$  is a length vector describing the impulse response of the channel during the OFDM symbol.

The output  $\mathbf{y}_{cp}$  has  $(L+v) + (v+1)-1 = L+2v$  samples. The first  $v$  samples of  $\mathbf{y}_{cp}$  contain interference from the preceding OFDM symbol and so are discarded. The last  $v$  samples disperse into the subsequent OFDM symbol, so also are discarded. This leaves exactly  $L$  samples for the desired output  $\mathbf{y}$ , which is precisely what is required to recover the  $L$  data symbols embedded in  $\mathbf{x}$ . Now it is to be justified that these  $L$  samples of  $\mathbf{y}$  will be equivalent to  $\mathbf{y} = \mathbf{h} \otimes \mathbf{x}$ . Proof is as follows using an inductive argument. Considering  $y_0$ , the first element in  $\mathbf{y}$ . As shown in Fig 2.5, owing to the cyclic prefix,  $y_0$  depends on the  $x_0$  and the circularly wrapped values of  $x_{L-v}, \dots, x_{L-1}$ .

That is:

$$\begin{aligned} y_0 &= h_0 x_0 + h_1 x_{L-1} + \dots + h_v x_{L-v} \\ y_1 &= h_0 x_1 + h_1 x_0 + \dots + h_v x_{L-v+1} \\ &\cdot \\ &\cdot \\ y_{L-1} &= h_0 x_{L-1} + h_1 x_{L-2} + \dots + h_v x_{L-v-1} \end{aligned} \quad (2.9)$$

From inspecting Eqn (2.2), it is seen that this is exactly the value of  $y_0, y_1, \dots, y_{L-1}$ , resulting from  $\mathbf{y} = \mathbf{x} \otimes \mathbf{h}$ . Thus, by using a circular convolution, a cyclic prefix that is at least as long as the channel duration allows the channel output  $\mathbf{y}$  to be decomposed into a simple multiplication of the channel frequency response  $\mathbf{H} = \text{DFT}\{\mathbf{h}\}$  and the channel frequency domain input,  $\mathbf{X} = \text{DFT}\{\mathbf{x}\}$ .

The cyclic prefix, although elegant and simple, is not entirely free. It comes with both a bandwidth and power penalty. Since  $v$  redundant symbols are sent, the required bandwidth for OFDM increases from  $B$  to  $(L + v / L)B$ . Similarly, an additional  $v$  symbol must be counted against the transmit-power budget. Hence, the cyclic prefix carries a power penalty of  $10 \log (L + v / L)$  dB in addition to the bandwidth penalty. In summary, the use of the cyclic prefix entails data rate and power losses that are given as:

$$\text{Rate Loss} = \text{Power Loss} = \frac{L}{L+v}$$

The “wasted” power has increased importance in an interference-limited wireless system, causing interference to neighboring users.

It is to be noted that for  $L \gg v$ , the inefficiency owing to the cyclic prefix can be made arbitrarily small by increasing the number of subcarriers. As with most system design problems, desirable properties, such as efficiency, must be traded off against cost and required tolerances.

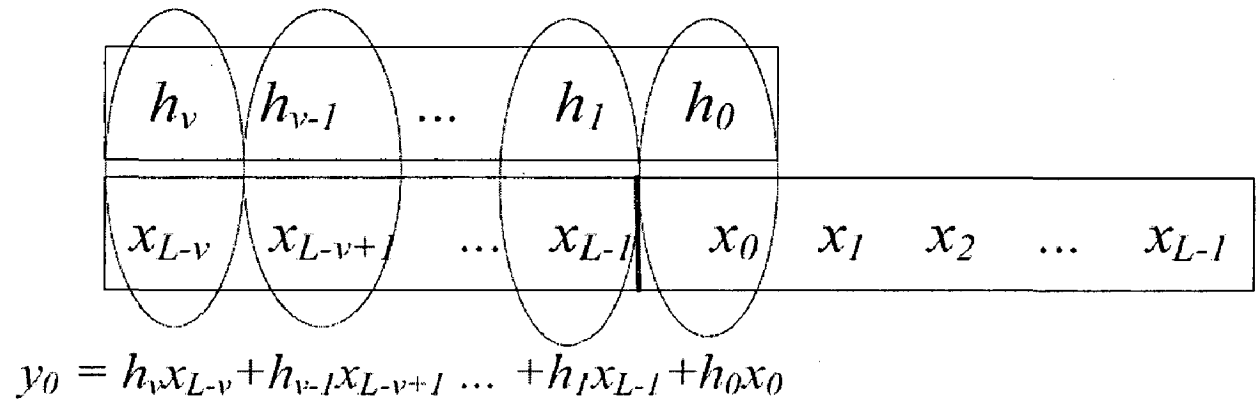


Figure 2.5 Circular convolution created by OFDM cyclic prefix [4]

### 2.2.4 Frequency Equalization

In order for the received symbols to be estimated, the complex channel gains for each subcarrier must be known, which corresponds to knowing the amplitude and phase of the subcarrier. For modulation techniques, such as QPSK, that don't use the amplitude to transmit information, only the phase information is sufficient.

After the FFT is performed, the data symbols are estimated using a one-tap frequency domain equalizer, or FEQ, as

$$\hat{X}_1 = \frac{Y_1}{H_1} \tag{2.10}$$

Where,  $H_1$  is the complex response of the channel at the frequency  $f_c + (l-1)\Delta f$ , and therefore it both corrects the phase and equalizes the amplitude before the decision device. It should be noted that although the FEQ inverts the channel, there is no problematic noise enhancement or coloring, since both the signal and the noise will have their powers directly scaled by  $\frac{1}{|H_1|^2}$ .

### 2.2.5 An OFDM Block Diagram

A review the steps in using OFDM communication system are shown in Fig 2.6. In OFDM, the encoding and decoding are done in the frequency domain, where  $\mathbf{X}$ ,  $\mathbf{Y}$ , and  $\hat{\mathbf{X}}$  contain the  $L$  transmitted, received, and estimated data symbols.

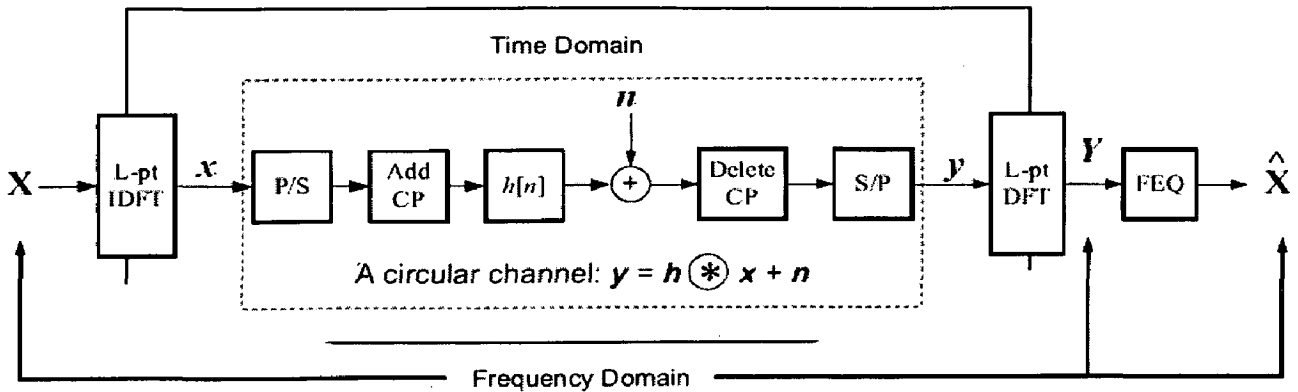


Figure 2.6 An OFDM system in vector notation [4]

1. The first step is to break a wideband signal of bandwidth  $B$  into  $L$  narrowband signals (subcarriers), each of bandwidth  $B/L$ . This way, the aggregate symbol rate is maintained, but each subcarrier experiences flat fading, or ISI-free communication, as long as a cyclic prefix that exceeds the delay spread is used. The  $L$  subcarriers for a given OFDM symbol are represented by a vector  $\mathbf{X}$ , which contains the  $L$  current symbols.
2. In order to use a single wideband radio instead of  $L$  independent narrowband radios, the subcarriers are modulated using an IFFT operation.
3. In order for the IFFT/FFT to decompose the ISI channel into orthogonal subcarriers, a cyclic prefix of length  $v$  must be appended after the IFFT operation. The resulting  $L+v$  symbols are then sent in serial through the wideband channel.
4. At the receiver, the cyclic prefix is discarded, and the  $L$  received symbols are demodulated, using an FFT operation, which results in  $L$  data symbols, each of the form  $Y_1 = H_1 X_1 + N_1$  for subcarrier 1.
5. Each subcarrier can then be equalized via an FEQ by simply dividing by the complex channel gain  $H[i]$  for that subcarrier. This results in  $\hat{X}_1 = X_1 + \frac{N_1}{H_1}$ .

# Chapter 3

## MIMO and Coding

In radio, multiple-input and multiple-output, or MIMO, is the use of multiple antennas at both the transmitter and receiver to improve communication performance [9]. It is one of several forms of Smart Antenna Technology. In this Chapter, MIMO techniques like Maximum Ratio Combining and Space Time Codes are [10,11] discussed.

### 3.1 Classical Maximal-Ratio Receive Combining (MRRC) Scheme

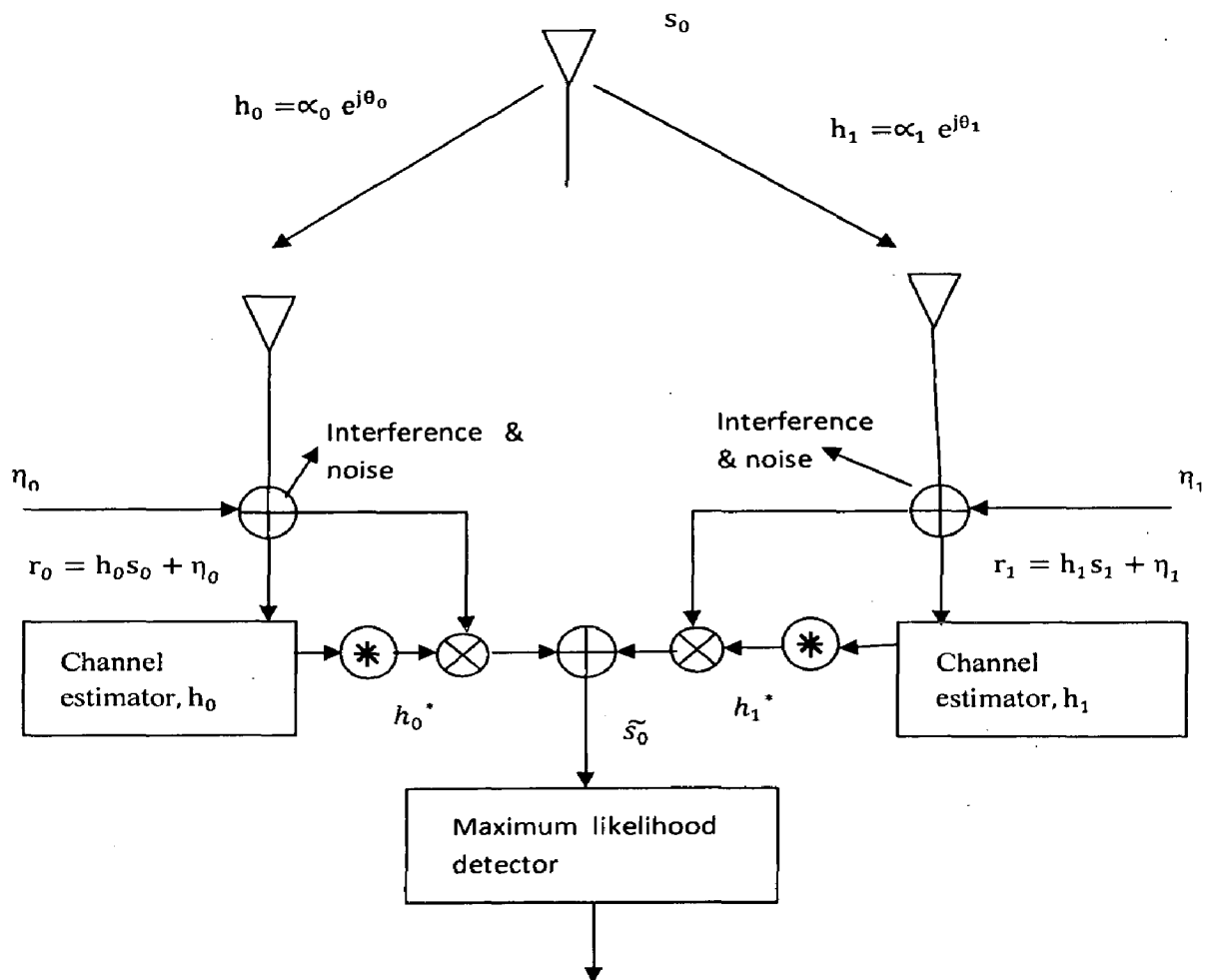


Figure 3.1 Classical MRRC scheme [10]

At a given time, a signal  $s_0$  is sent from the transmitter. The channel including the effects of the transmit chain, the air link, and the receive chain may be modeled by the



complex multiplicative distortion composed of a magnitude response and a phase response. Fig 3.1 shows the baseband representation of the classical two-branch MRRC. The channel between the transmit antenna and the receive antenna zero is denoted by  $h_0$  and between the transmit antenna and the receive antenna one is denoted by  $h_1$  where

$$\begin{aligned} h_0 &= \alpha_0 e^{j\theta_0} \\ h_1 &= \alpha_1 e^{j\theta_1} \end{aligned} \quad (3.1)$$

Complex Noise is added at the two receivers. The resulting received baseband signals are

$$\begin{aligned} r_0 &= h_0 s_0 + \eta_0 \\ r_1 &= h_1 s_0 + \eta_1 \end{aligned} \quad (3.2)$$

where  $\eta_0$  and  $\eta_1$  represent complex noise. Assuming  $\eta_0$  and  $\eta_1$  are Gaussian distributed, the maximum likelihood decision rule at the receiver for these received signals is to choose signal  $s_i$  if and only if (iff)

$$d^2(r_0, h_0 s_i) + d^2(r_1, h_1 s_i) \leq d^2(r_0, h_0 s_k) + d^2(r_1, h_1 s_k) \quad \forall i \neq k \quad (3.3)$$

The receiver combining scheme for two-branch MRRC is as follows:

$$\tilde{s}_0 = h_0^* r_0 + r_1 h_1^* \quad (3.4)$$

Using Eqn (3.3) and using Eqn (3.4) we get choose  $s_i$  iff

$$(\alpha_0^2 + \alpha_1^2 - 1)|s_i|^2 + d^2(\tilde{s}_0, s_i) \leq (\alpha_0^2 + \alpha_1^2 - 1)|s_k|^2 + d^2(\tilde{s}_0, s_k) \quad \forall i \neq k \quad (3.5)$$

If suppose we have

$$|s_i|^2 = |s_k|^2 = E_s \quad \forall i, k \quad (3.6)$$

Where  $E_s$  is the energy of the signal. Therefore, for PSK signals, the decision rule in Eqn (3.5) may be simplified to choose  $s_i$  iff

$$d^2(\tilde{s}_0, s_i) \leq d^2(\tilde{s}_0, s_k) \quad \forall i, k \quad (3.7)$$

The maximal-ratio combiner may then construct the signal  $\tilde{s}_0$ , as shown in Fig. 3.1, so that the maximum likelihood detector may produce  $\hat{s}_0$ , which is a maximum likelihood estimate of  $s_0$ .

### 3.2 Alamouti Transmit Diversity Schemes

#### A: Two-Branch Transmit Diversity with One Receiver

As discussed previously, MRC uses the multiple antennas at the Receiver, there is other way round to impart diversity to the Transmission at the Transmitter proposed by Alamouti [10].

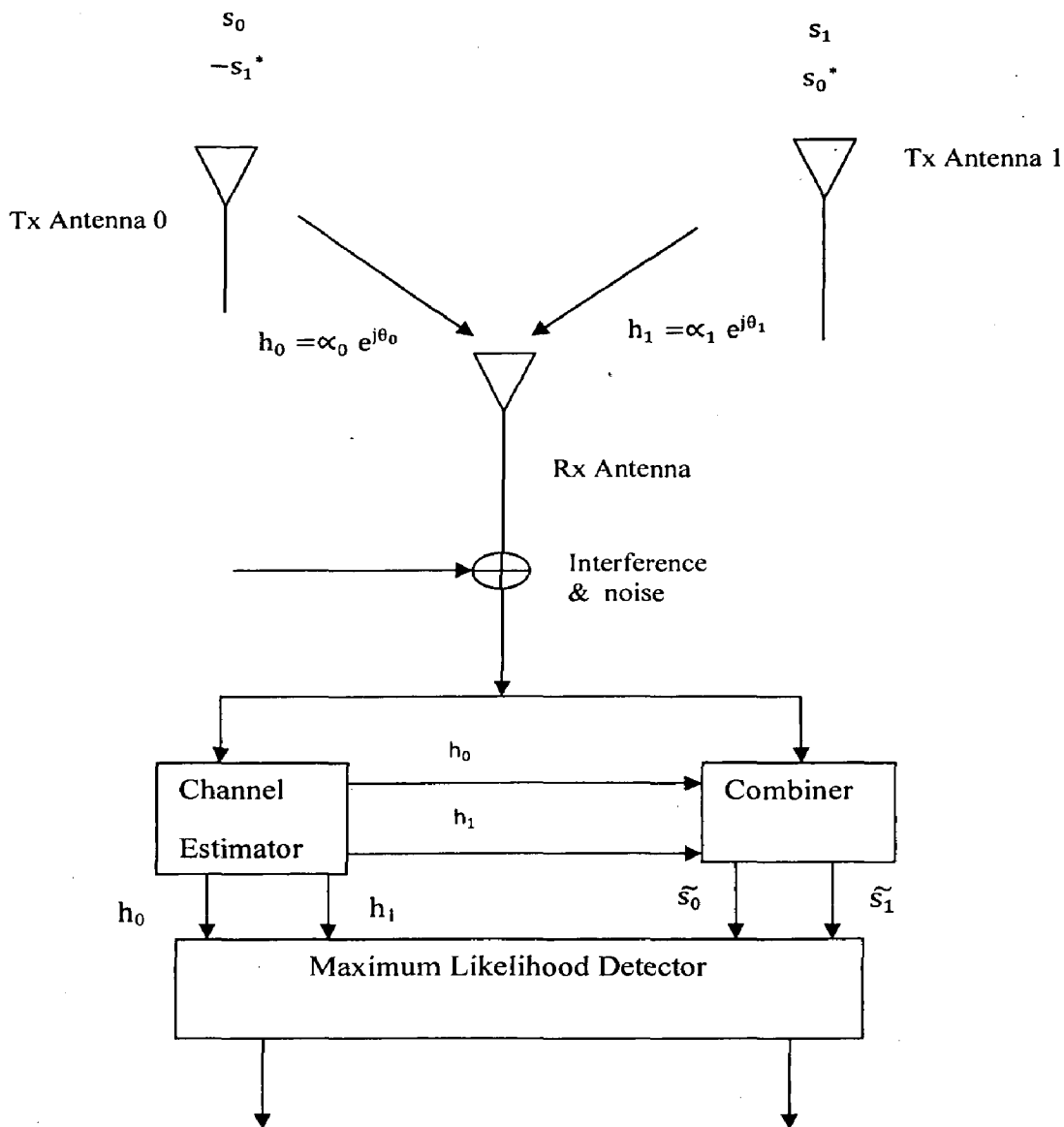


Figure 3.2 Alamouti two by one transmit diversity scheme [10]

In the Fig 3.2 baseband representation of the new two branch transmit diversity scheme is shown. The scheme uses two transmit antennas and one receive antenna and are defined by the following three functions:

- Encoding and transmission sequence of information symbols at the transmitter,
- Combining scheme at the receiver, and
- Decision rule for maximum likelihood detection

1) The Encoding and Transmission Sequence: At a given symbol period, two signals are simultaneously transmitted from the two antennas. The signal transmitted from antenna zero is denoted by  $s_0$  and from antenna one by  $s_1$ . During the next symbol period signal  $(-s_1^*)$  is transmitted from antenna zero, and signal  $s_0^*$  is transmitted from antenna one where  $*$  is the complex conjugate operation. This sequence is shown in Table I.

In Table I, the encoding is done in space and time (space–time coding). The encoding, however, may also be done in space and frequency. Instead of two adjacent symbol periods, two adjacent carriers may be used (space–frequency coding).

Table 3.1: symbol representation of antennas with time [11]

	Antenna 1	Antenna 2
Time 't'	$s_0$	$s_1$
Time 't+T <sub>s</sub> '	$-s_1^*$	$s_0^*$

The channel at time may be modeled by a complex multiplicative distortion  $h_0(t)$  for transmit antenna zero and  $h_1(t)$  for transmit antenna one. Assuming that fading is constant across two consecutive symbols, received symbols can be written as:

$$\begin{aligned}
 r_0 &= r(t) = h_0 s_0 + h_1 s_1 + \eta_0 \\
 r_1 &= r(t + T_s) = -h_0 s_1^* + h_1 s_0^* + \eta_1
 \end{aligned} \tag{3.8}$$

2) The Combining Scheme: The Combiner is shown in Fig 3.2 builds the following combining signals that are sent to the Maximum Likelihood detector:

$$\begin{aligned}
 \tilde{s}_0 &= h_0^* r_0 + h_1 r_1^* \\
 \tilde{s}_1 &= h_1^* r_0 - h_0 r_1^*
 \end{aligned} \tag{3.9}$$

It is important to note that this combining scheme is different from the MRRC in Eqn (3.5). Substituting Eqn (3.7) and Eqn (3.8) into Eqn (3.9) we get

$$\begin{aligned}\tilde{s}_0 &= (\alpha_0^2 + \alpha_1^2)s_0 + h_0^* \eta_0 + h_1 \eta_1^* \\ \tilde{s}_1 &= (\alpha_0^2 + \alpha_1^2)s_1 - h_0 \eta_1^* + h_1^* \eta_0\end{aligned}\tag{3.10}$$

3) The Maximum Likelihood Decision Rule: These combined signals are then sent to the maximum likelihood detector which, for each of the signals and, uses the decision rule expressed in Eqn (3.5) or Eqn (3.7) for PSK signals. The resulting combined signals in Eqn (3.10) are equivalent to that obtained from two-branch MRRC in Eqn (3.3). The only difference is phase rotations on the noise components which do not degrade the effective SNR. Therefore, the resulting diversity order from the two-branch transmit diversity scheme with one receiver is equal to that of two-branch MRRC.

*B. Two-Branch Transmit Diversity with multiple Receivers:*

There may be applications where a higher order of diversity is needed and multiple receive antennas at the remote units are feasible. In such cases, it is possible to provide a diversity order of  $2M$  with two transmit and  $M$  receive antennas.

The encoding and transmission sequence of the information symbols for this configuration is identical to the case of a single receiver, shown in Table 3.1.

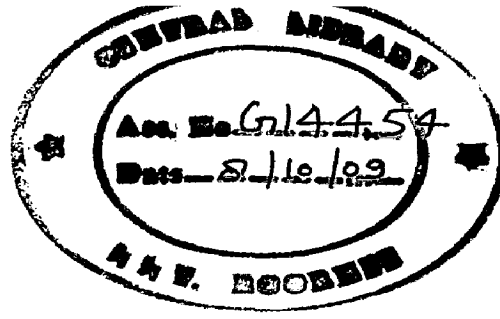
Table 3.2: Definition of Channels between Transmitter and Receiver [11]

	Antenna 1	Antenna 2
TX Antenna 0	$h_0$	$h_2$
TX Antenna 1	$h_1$	$h_3$

Table 3.3: Notation for received signals and Transmit antennas [11]

	Antenna 1	Antenna 2
Time 't'	$r_0$	$r_2$
Time 't+T <sub>s</sub> '	$r_1$	$r_3$

In the Table 3.2, the channels between the transmit and receive antennas are defined, and Table 3.3 defines the notation for the received signal at the two receive antennas.



Where

$$\begin{aligned}
 r_0 &= h_0 s_0 + h_1 s_1 + \eta_0 \\
 r_1 &= -h_0 s_0^* + h_1 s_0^* + \eta_1 \\
 r_2 &= h_2 s_0 + h_3 s_1 + \eta_2 \\
 r_3 &= -h_2 s_1^* + h_3 s_0^* + \eta_3
 \end{aligned} \tag{3.11}$$

$\eta_0, \eta_1, \eta_2,$  and  $\eta_3$  are complex random variables representing receiver complex noise.

The combiner similar to that in Fig 3.2 builds the following two signals that are sent to the maximum likelihood detector (after substituting the appropriate equations):

$$\begin{aligned}
 \tilde{s}_0 &= (\alpha_0^2 + \alpha_1^2 + \alpha_2^2 + \alpha_3^2) s_0 + h_0^* \eta_0 + h_1 \eta_1^* + h_2^* \eta_2 + h_3 \eta_3^* \\
 \tilde{s}_1 &= (\alpha_0^2 + \alpha_1^2 + \alpha_2^2 + \alpha_3^2) s_1 - h_0 \eta_1^* + h_1^* \eta_0 + h_3^* \eta_2 - h_2 \eta_3^*
 \end{aligned} \tag{3.12}$$

After Maximum likelihood detector  $s_i$  is chosen iff

$$\begin{aligned}
 (\alpha_0^2 + \alpha_1^2 + \alpha_2^2 + \alpha_3^2 - 1) |s_i|^2 + d^2(\tilde{s}_0, s_i) &\leq \\
 (\alpha_0^2 + \alpha_1^2 + \alpha_2^2 + \alpha_3^2 - 1) |s_k|^2 + d^2(\tilde{s}_0, s_k) \quad \forall i \neq k
 \end{aligned} \tag{3.13}$$

For PSK signals,  $s_i$  is chosen iff

$$d^2(\tilde{s}_0, s_i) \leq d^2(\tilde{s}_0, s_k) \quad \forall i \neq k \tag{3.14}$$

Similarly, for  $s_1$ , using the decision rule for choosing  $s_i$ , we have

$$\begin{aligned}
 (\alpha_0^2 + \alpha_1^2 + \alpha_2^2 + \alpha_3^2 - 1) |s_i|^2 + d^2(\tilde{s}_1, s_i) &\leq \\
 (\alpha_0^2 + \alpha_1^2 + \alpha_2^2 + \alpha_3^2 - 1) |s_k|^2 + d^2(\tilde{s}_1, s_k) \quad \forall i \neq k
 \end{aligned} \tag{3.15}$$

$$\text{For PSK } d^2(\tilde{s}_1, s_i) \leq d^2(\tilde{s}_1, s_k) \quad \forall i \neq k \tag{3.16}$$

It is to be noted that the combined signals from the two receive antennas are the simple addition of the combined signals from each receive antenna, i.e., the combining scheme is identical to the case with a single receive antenna. It may be concluded that, using two transmit and M receive antennas, combiner for each receive antenna can be used, and then simply add the combined signals from all the receive antennas to obtain the same diversity order as 2M branch MRRC. In stated other way, using two antennas at the transmitter, the scheme doubles the diversity order of systems with one transmit and multiple receive antennas.

A motivating configuration may be to employ two antennas at each side of the link, with a transmitter and receiver chain connected to each antenna to obtain a diversity order of four at both sides of the link.

### 3.3. Assumptions

- 1) Total transmit power from the two antennas for the new scheme is the same as the transmit power from the single transmit antenna for MRRC [11].
- 2) The amplitudes of fading from each transmit antenna to each receive antenna are mutually uncorrelated Rayleigh distributed and that the average signal powers at each receive antenna from each transmit antenna are the same.
- 3) The receiver has perfect knowledge of the channel.

### 3.4 Convolutional Coding

First introduced by Elias (1955), binary convolutional codes are one of the most popular forms of binary error correcting codes that have found numerous applications: wireless Communications (IMT-2000, GSM, IS-95etc.), digital terrestrial and satellite communications and broadcasting systems and space communication systems [12]. Their most popular decoding method is the Viterbi algorithm (Viterbi 1967). It has been shown (Space Communications etc.) that convolutional codes, when combined with interleaving in a concatenated scheme, can perform very close to the Shannon limit.

A convolutional code is an error correcting code that processes information serially or, continuously. A convolutional encoder has memory, which means that the output symbols depend not only on the input symbols but also on previous inputs and/or outputs .

In the Fig 3.3, represents  $\frac{1}{2}$  rate Convolutional encoder with Constraint Length K (memory length +1), Feed Forward encoder with single input and two outputs.

The Trellis Structure has 4 distinct states which are useful in determining the optimum input sequence while decoding with Viterbi Decoding (VD) [13].

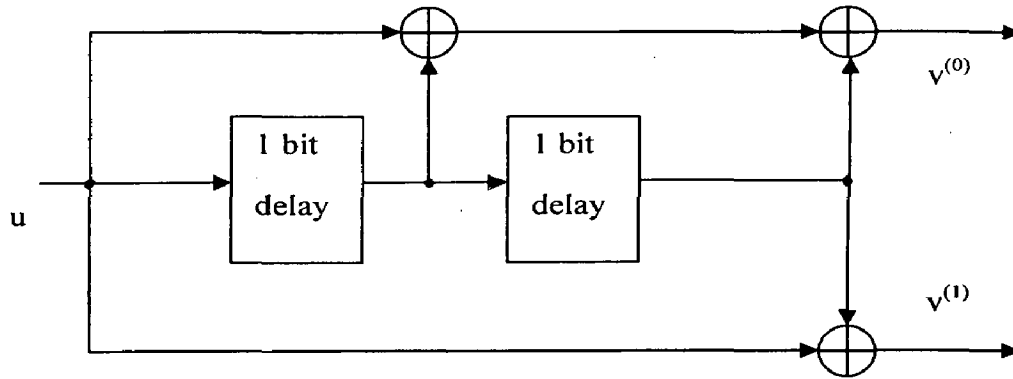


Figure 3.3 Feed Forward Convolutional Encoder (Memory length 2, rate .5) [12]

Generating polynomials are the polynomials which determine the relation of output sequences with that of input sequence. For the Fig 3.3 Generating Polynomials (in binary) are (111) and (101) for  $v^{(0)}$  and  $v^{(1)}$  respectively. The outputs are realized as Convolution of the input with these generating Polynomials and taking Modulo 2 division [14].

#### *Punctured Convolutional Codes*

Puncturing is the process of systematically deleting, some output bits of a low-rate encoder. Since the trellis structure of the low-rate encoder remains the same, the number of information bits per sequence does not change. As a result, the output sequences belong to a higher-rate Punctured Convolutional (PC) code.

The Puncturing Matrix  $\mathbf{P} = \begin{bmatrix} 1 & 1 \\ 1 & 0 \end{bmatrix}$  transmits the upper part of the output sequence as it is and since the binary multiplication of both ones puts it same. For the lower out sequence alternative symbols are dropped for transmission, making the 1/2 code rate to 2/3.

In order to achieve decoding of a PC code using the VD of the low-rate code is by inserting “deleted” symbols in the positions that were not sent. This process is known as depuncturing. The “deleted” symbols are marked by a special flag. This can be done, by using an additional bit and setting it to 1 in the position of an erased bit. If a position is flagged, then the corresponding received symbol is not taken into account in the branch metric computation.

# Chapter 4

## Link Adaptation for Time Varying Multipath Channels

---

Link Adaptation (LA) algorithm generally chooses a suitable MCS to increase the throughput of a system while maintaining some Quality of Service (QoS) objectives. The QoS objectives are, Block loss, Connectivity, Block delivery delay etc. In this dissertation, the QoS objective is to verify Block Error Rate (BLER) of a particular MCS (which determines the statistics of retransmissions and ultimately determines the throughput and latency of a system) [15, 16]. Thus, LA algorithm with QoS objective will select a suitable MCS value by full filling the target BLER requirement.

### 4.1 Slow and Fast Link Adaptation

When the CSI is not available at the receiver, then a simple approach is to estimate BLER by simply dividing the number of erroneous blocks by a total number of received blocks for a given time period window. However, this approach requires a long time to converge especially at a low BLER. This kind of approach is known as Slow Link Adaptation (SLA) because it takes a lot of time to accumulate enough blocks to estimate BLER. SLA is usually stacked in the MAC layer.

If CSI is available at the receiver, a better and an accurate estimation of BLER can also be found which will converge fast. Thus, this kind of LA can be defined as Fast Link Adaptation (FLA) which estimates a suitable MCS that full fills the QoS constraint for a given CSI. Thereafter, the receiver recommends the estimated MCS via feedback to the transmitter so that the transmitter can transmit data at highest possible rate according to the current channel conditions. Furthermore, the CSI considered in this thesis is channel matrix ( $\mathbf{H}$ ) and noise variance ( $N_0$ ) (or post-processing SINR) available per subcarrier.

### 4.2 Channel Modeling

In order to evaluate the performance of the developed communication system, an accurate description of the wireless channel is required to address its propagation environment [17]. The radio architecture of a communication system plays very



significant role in the modeling of a channel. The wireless channel is characterized mainly by:

- Path loss.
- Multipath delay spread.
- Fading Characteristics.
- Doppler spread and.
- Cochannel and Adjacent channel interference.

All the model parameters are random in nature and only a statistical characterization of them is possible, i.e. in terms of the mean and variance value. They are dependent upon terrain, tree density, antenna height and beam width, wind speed and time of the year.

#### *Path loss*

Path loss is affected by several factors such as terrain contours, different environments (urban or rural, vegetation and foliage), propagation medium (dry or moist air), the distance between the transmitter and the receiver, the height and location of their antennas, etc.

#### *Multipath Delay Spread*

Due to the Non Line of Sight (NLOS) propagation nature of the signal, multipath delay spread is to be included. It results due to the scattering nature of the environment. Delay spread is a parameter used to signify the effect of multipath propagation. It depends on the terrain, distance, antenna directivity and other factors. The rms delay spread value can span from tens of nano seconds to micro seconds.

#### *Fading Characteristics*

In a multipath propagation environment, the received signal experiences fluctuation in its amplitude, phase and angle of arrival. The effect is described by the term multipath fading. The important one, Small scale fading refers to the dramatic changes in signal amplitude and phase that can be experienced as a result of small changes (as small as a half wavelength) in the spatial positioning between a receiver and a transmitter. Small scale fading is called Rayleigh fading if there are multiple reflective paths that are large in number and there is no line of sight signal component, the envelope of

such a received signal is statistically described by a Rayleigh Probability Density Function (pdf). When a dominant non fading signal component is present, such as a line of sight propagation path, the small scale fading envelope is described by a Rician pdf. In other words, the small scale fading statistics are said to be Rayleigh whenever the line of sight path is blocked, and Rician otherwise. The key parameter of Rician distribution is the K factor, defined as the ratio of the direct component power and the scatter component power.

### *Doppler Spread*

In fixed wireless access, a Doppler frequency shift is induced on the signal due to movement of the objects in the environment. Doppler spectrum of fixed wireless channel differs from that of mobile channel. It is found that the Doppler is in the 0.12 Hz frequency range for fixed wireless channel [15]. Along with the above channel parameters, coherence distance, co-channel interference, antenna gain reduction factor should be addressed for channel modeling.

## **4.3 Derivation of the basic Exponential ESM**

The exponential ESM is derived based on the Union-Chernoff bound of error probabilities [18]. The union bound for coded binary transmission and maximum-likelihood decoding is given by

$$P_e(\gamma) \leq \sum_{d=d_{\min}}^{\infty} \alpha_d P_2(d, \gamma) \quad (4.1)$$

where,

$\gamma$  is the channel symbol SNR,

$d_{\min}$  is the minimum distance of the binary code,

$\alpha_d$  is the number of code words with hamming weight  $d$ , and

$P_2(d, \gamma)$  is the Pair-wise Error Probability (PEP) assuming a certain Hamming distance  $d$  and a certain symbol SNR  $\gamma$ .

For BPSK transmission over an AWGN channel and using Chernoff-bounding techniques, the PEP can be upper bounded according to

$$P_2(d, \gamma) \leq Q(\sqrt{2\gamma d}) \leq e^{-\gamma d} \triangleq P_{2,\text{Chernoff}}(d, \gamma) = [P_{2,\text{Chernoff}}(1, \gamma)]^d \quad (4.2)$$

The last part of the above expression implies that the Chernoff-bounded PEP is directly given by the Chernoff-bounded (uncoded) symbol-error probability [19]. Thus, the Chernoff-bounded error probability  $P_{e,\text{Chernoff}}(\gamma)$  only depends on the weight distribution of the code and the Chernoff-bounded symbol-error probability  $P_{2,\text{Chernoff}}(1, \gamma)$  according to

$$P_e(\gamma) \leq \sum_{d=d_{\min}}^{\infty} \alpha_d P_2(d, \gamma) \leq \sum_{d=d_{\min}}^{\infty} \alpha_d [P_{2,\text{Chernoff}}(1, \gamma)]^d \triangleq P_{e,\text{Chernoff}}(\gamma) \quad (4.3)$$

The basic principles for the Union Chernoff bound for a multi-state channel, i.e. a channel where different coded bits are subject to different SNR, is explained with the simple example of a 2-state channel. The principles are then straightforwardly extended to the general multi-state channel.

The 2-state channel is characterized by an SNR vector given by  $\boldsymbol{\gamma} = [\gamma_1, \gamma_2]$  where, in general, the two states  $\gamma_1$  and  $\gamma_2$  occur with probability  $p_1$  and  $p_2$  respectively. Furthermore, the two SNR values are assumed to be independent from each other, which require a corresponding interleaver in practice.

Now the case of two arbitrary code words with hamming distance  $d$  is seen. The SNR value, either  $\gamma_1$  or  $\gamma_2$ , associated with each of the  $d$  differing symbols depends on the respective symbol position. That means that the exact PEP for these two code words in case of a 2-state channel does not only depend on the distance  $d$ , but also on the position of the  $d$  differing symbols. Thus the union bound approach in the classical sense that all code-word pairs are compared would require detailed code knowledge about the bit positions. Instead, in this case the mean PEP, averaged over all possible positions of the  $d$  differing symbols, is used. This is equivalent to average over all possible cases how the SNR values  $\gamma_1$  and  $\gamma_2$  may be distributed among the  $d$  differing symbols. Hence, the Chernoff bounded PEP can be expressed as

$$P_{2,\text{Chernoff}}(d, [\gamma_1, \gamma_2]) = \sum_{i=0}^d \binom{d}{i} p_1^i p_2^{d-i} e^{-(i\gamma_1 + (d-i)\gamma_2)} = (p_1 e^{-\gamma_1} + p_2 e^{-\gamma_2})^d \quad (4.4)$$

where  $\binom{d}{i}$  is  $dC_i$ . The binomial theorem has been used to arrive at the final expression. To clarify the second expression,  $p_1^i p_2^{d-i}$  represents the probability that  $i$  of the  $d$  differing symbols are associated with SNR  $\gamma_1$  and the residual  $(d-i)$  symbols are associated with SNR  $\gamma_2$ .

There are  $\binom{d}{i}$  such events and  $e^{-(i\gamma_1+(d-i)\gamma_2)}$  is the Chernoff-bounded PEP for such an event. It should be noted that the term  $(p_1 e^{-\gamma_1} + p_2 e^{-\gamma_2})$  is the averaged Chernoff-bounded symbol-error probability for the 2-state channel. Therefore, the relationship found for the 1-state channels is also valid for the 2-state channel, i.e.

$$P_{2,\text{Chernoff}}(d, [\gamma_1, \gamma_2]) = [P_{2,\text{Chernoff}}(1, [\gamma_1, \gamma_2])]^d \quad (4.5)$$

Moreover, from the polynomial theorem, <sup>[18]</sup> it can be shown that the same is true for the general multi-state channel, characterized by a vector

$\boldsymbol{\gamma} = [\gamma_1, \gamma_2 \dots \gamma_N]$ , i.e.

$$P_{2,\text{Chernoff}}(d, \boldsymbol{\gamma}) = [P_{2,\text{Chernoff}}(1, \boldsymbol{\gamma})]^d \quad (4.6)$$

This feature of the Chernoff-bounded PEP is now exploited to derive the EESM. The goal is to find an effective SNR value  $\gamma_{\text{eff}}$  of an equivalent 1-state channel such that the Chernoff-bounded error probability equals the Chernoff-bounded error probability on the multi-state channel, i.e.

$$P_{e,\text{Chernoff}}(\gamma_{\text{eff}}) = P_{e,\text{Chernoff}}(\boldsymbol{\gamma}) \quad (4.7)$$

Due to the feature stated above, this can be achieved by matching the respective Chernoff-bounded symbol-error probabilities

$$P_{2,\text{Chernoff}}(1, \gamma_{\text{eff}}) = P_{2,\text{Chernoff}}(1, \boldsymbol{\gamma}) \quad (4.8)$$

Inserting the Chernoff-bound expressions directly gives the exponential ESM:

$$\gamma_{\text{eff}} = -\ln\left(\sum_{k=1}^N p_k e^{-\gamma_k}\right) \quad (4.9)$$

or, for the case of OFDM with N carriers and different SNR  $\gamma_k$  on each carrier:

$$\gamma_{\text{eff}} = -\ln\left(\frac{1}{N} \sum_{k=1}^N e^{-\gamma_k}\right) \quad (4.10)$$

## 4.4 A Generalized Exponential ESM

In above derivations, it has been assumed for binary transmission (BPSK). For QPSK modulation, the EESM becomes

$$\gamma_{\text{eff}} = -2 * \ln\left(\frac{1}{N} \sum_{k=1}^N e^{-\frac{\gamma_k}{2}}\right) \quad (4.11)$$

For higher-order modulation, such as 16QAM, it is not as straightforward to determine the exact expression for the EESM. The reason is that higher-order modulation in itself can be seen as a multistate channel from a binary-symbol transmission point-of-view. Instead, generalized EESM is stated including a parameter  $\beta$  that can be adjusted to match the ESM a specific combination of modulation scheme and coding rate [20]. A suitable value for the parameter  $\beta$  for each modulation scheme and/or coding rate of interest can then be from link-level simulations.

$$\gamma_{\text{eff}} = -\beta \cdot \ln\left(\frac{1}{N} \sum_{k=1}^N e^{-\frac{\gamma_k}{\beta}}\right) \quad (4.12)$$

## 4.5 Link Abstraction

*General Per-Tone Model [20]:*

The signal model for the received signal per tone is given by

$$\mathbf{y} = \sqrt{P_0} \mathbf{H}^{(0)} \mathbf{x}_0 + \sum_{k=1}^K \sqrt{P_k} \mathbf{H}^{(k)} \mathbf{x}_k + \mathbf{n} \quad (4.13)$$

where  $\mathbf{y}$  is a  $N_r \times 1$  receive vector,  $\mathbf{x}_k$  is a  $N_t \times 1$  transmit vector,  $\mathbf{n}$  is  $N_r \times 1$  noise vector (with zero mean and variance  $\sigma^2$ , circularly symmetric normal distributed entries),  $\mathbf{H}_k$  is a  $N_r \times N_t$  channel matrix,  $K$  is the number of interferers, and  $P_k$  is the received power from  $k^{\text{th}}$  BS given by

$$P_k = P_T G_k \frac{10^{X_k/10}}{L(d_k)} \quad (4.14)$$

where  $P_T$  is the transmit power,  $X_k$  the log-normal shadowing,  $L(d_k)$  is the path loss at distance  $d_k$ , and  $G_k$  is the aggregate antenna gain. Without loss of generality it is assumed that the  $k=0^{\text{th}}$  BS is the desired BS. For a linear receiver, the postreceiver signal is obtained by premultiplying the received input,  $\mathbf{y}$ , by the vector/matrix  $\mathbf{w}^*$

$$\mathbf{z} = \mathbf{w}^* \mathbf{y} \quad (4.15)$$

The choice of  $\mathbf{w}$  depends on the receiver scheme, i.e. Maximal Ratio Combining (MRC) or linear Minimum Mean Squared Error (MMSE). The post-receiver SINR per tone is given by

$$\Gamma = \frac{P_0 |\mathbf{w}^* \mathbf{H}^{(0)}|^2}{\sum_{k=1}^K P_k |\mathbf{w}^* \mathbf{H}^{(k)}|^2 + \|\mathbf{w}\|^2 \sigma_n^2}, \quad (4.16)$$

which can be rewritten as

$$\Upsilon = \frac{P_0 f(\mathbf{H}^{(0)})}{\sum_{k=1}^K P_k g(\mathbf{H}^{(k)}) + \sigma_n^2} \quad (4.17)$$

It is to be noted that  $f(\cdot)$  and  $g(\cdot)$  denote the receiver processing on the signal and interferer, respectively. For SISO case, considering MRC Receiver Scheme, replacing  $\mathbf{H}$  with scalar appropriately, Eqn (4.17) reduces to

$$\Upsilon = \frac{P_0 |\mathbf{H}^{(0)}|^2}{\sum_{k=1}^K P_k |\mathbf{H}^{(k)}|^2 + \sigma_n^2} \quad (4.18)$$

#### 4.6 Calibration of $\beta$ [21, 22]

*Assumptions and Parameters:* All simulations were carried out with floating point calculations, assuming ideal channel estimation. All calibrations were done with Convolutional Codes, with variable Modulation and coding rates, also for variable Block sizes.

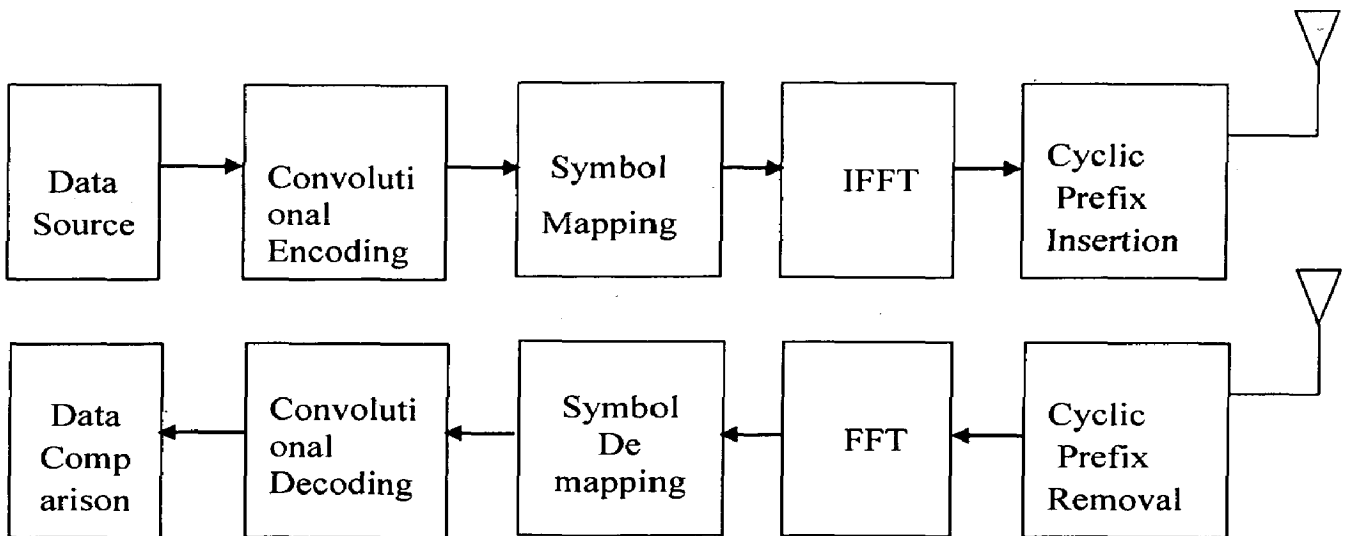


Figure 4.1 Block Diagram for Transmitter (above) and Receiver (below) Blocks using OFDM.

To calibrate  $\beta$  for a given MCS level, several realizations were created from different channel models. For each channel realization, the BLER was determined by simulation. This leads to a mapping from  $\gamma$  to BLER. Using an AWGN reference curve for the same MCS level, this BLER is mapped to an AWGN equivalent SNR which is in turn used to determine  $\beta$ . This intern leads to the expression for  $\beta$ :

$$\beta = \arg \min_{\beta} \|\text{SNR}_{\text{AWGN}} - \Gamma_{\text{eff}}(\beta)\| \quad (4.19)$$

Where  $\text{SNR}_{\text{AWGN}} = [ \text{SNR}_{\text{AWGN}, 1}, \text{SNR}_{\text{AWGN}, 2}, \dots, \text{SNR}_{\text{AWGN}, n} ]$  and  $\Gamma_{\text{eff}}(\beta) = [ \gamma_{\text{eff}, 1}(\beta), \gamma_{\text{eff}, 2}(\beta), \dots, \gamma_{\text{eff}, n}(\beta) ]$  are the vectors with elements corresponding to several Channel realizations.

Different metrics could be proposed for (4.19). It could be chosen to minimize the difference measured in SNR or in BLER, and both of these could be measured on a logarithmic (dB) scale or on a linear scale.

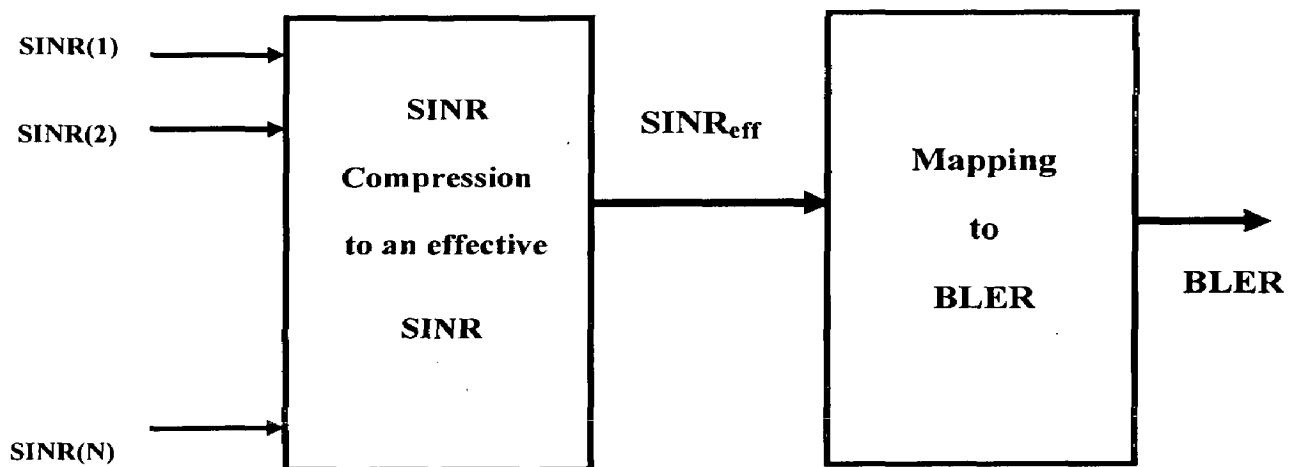


Figure 4.2 Method of EESM showing instantaneous SINR Mapping to BLER

The EESM mapping is less sensitive in the range of low SNR's (as they are all mapped to BLER = 1). The range of interest for 802.16 is where the BLER is roughly between the values of 0.02 and 0.002. Furthermore, measuring accurate BLER in the range lower than 0.001 is very time consuming since the number of frames required to simulate them (for each channel realization) with reasonable accuracy is approximately 100/ BLER.

After evaluating different metrics, metrics based on SNR and BLER turned out to have equivalent behavior (in producing similar  $\beta$ 's). The dB scale is more homogeneous over the range of interest. Using the linear scale, more weight is put on the low SNR's, which produces vague results [23]. Taking this into account, least squares with respect to SNR (dB) is the preferable metric for both implementation and performance.



# Chapter 5

## Simulation Results

---

### 5.1 Simulation of STCs and EESM Scheme:

*For implementing Space Time Codes:*

Performance is evaluated for while considering SNRs over range of interest (15/BER). Averaging has been done generating Rayleigh channel in 10 simulations. Random binary data is directly transmitted after modulation in a SISO case and MRRC cases. When considering Alamouti schemes data is copied to each transmitter and the symbol transmitted sequence at a transmitter is decided by the combining scheme given by Alamouti. In a two Transmitting antenna case, the transmitted power is halved and equally divided for each symbol. The channel is generated every time using two `randn()` functions independently. This information is available at the receiver. AWGN is added to transmitted sequence for given SNR. Combining schemes for respective antenna combinations are given in chapter 3. It is to be observed through simulations, even though the transmitter power is same with increase in transmitting antennas, the scheme performs better compared to SISO. With increase in total (transmit and receive) system performs still better.

*For EESM Scheme:*

The main aim of this thesis is to provide the desired beta values for common MCS levels. The main steps to get the best beta value for a specific MCS level are described in details in this section.

The steps to obtain beta value are as follows. First, generate an AWGN curve for a specific MCS (4 QAM .5 Rate etc) level. Second, calculate the SINR per tone (given in chapter 4) values for the same MCS level using the desired channel model (for instance Ped A etc). Many channel realizations are required, and SINR per tone values should be converted to one scalar value to represent the channel SINR using EESM formula.

The third step is to compare the two values gained from the previous steps (SINR EESM and SNR AWGN). The comparisons for many SNR-pair values will yield a

mean squared difference for a given beta value. The beta value that gives the minimum difference is selected as the optimal value.

In the first step the AWGN channel model is used to generate the reference curve. The BLER values that are of interest are those that result in a satisfactory operation. This range includes small BLER values close to zero.

It is to be observed that EESM scheme performs well with BPSK, 4 QAM, and the accuracy decreases with increasing in higher order modulation schemes (16 QAM, 64QAM).

**System parameters:**

- Modulation : 4, 16, 64 QAM
- No. of subcarriers : 1024
- Coding Rate : .5, .75
- Band width : 10 MHz

Table 5.1: Delay and Power value for Ped A and Ped B Channel Models

Tap	Channel A		Channel B	
	Relative Delay (ns)	Average Power (db)	Relative Delay (ns)	Average Power (db)
1	0	0	0	0
2	110	-9.7	200	-9
3	190	-19.2	800	-4.9
4	410	-22.8	1200	-8.0
5	-	-	2300	-7.8
6	-	-	3700	-23.9

## 5.2 Flow chart for implementing Space Time Codes

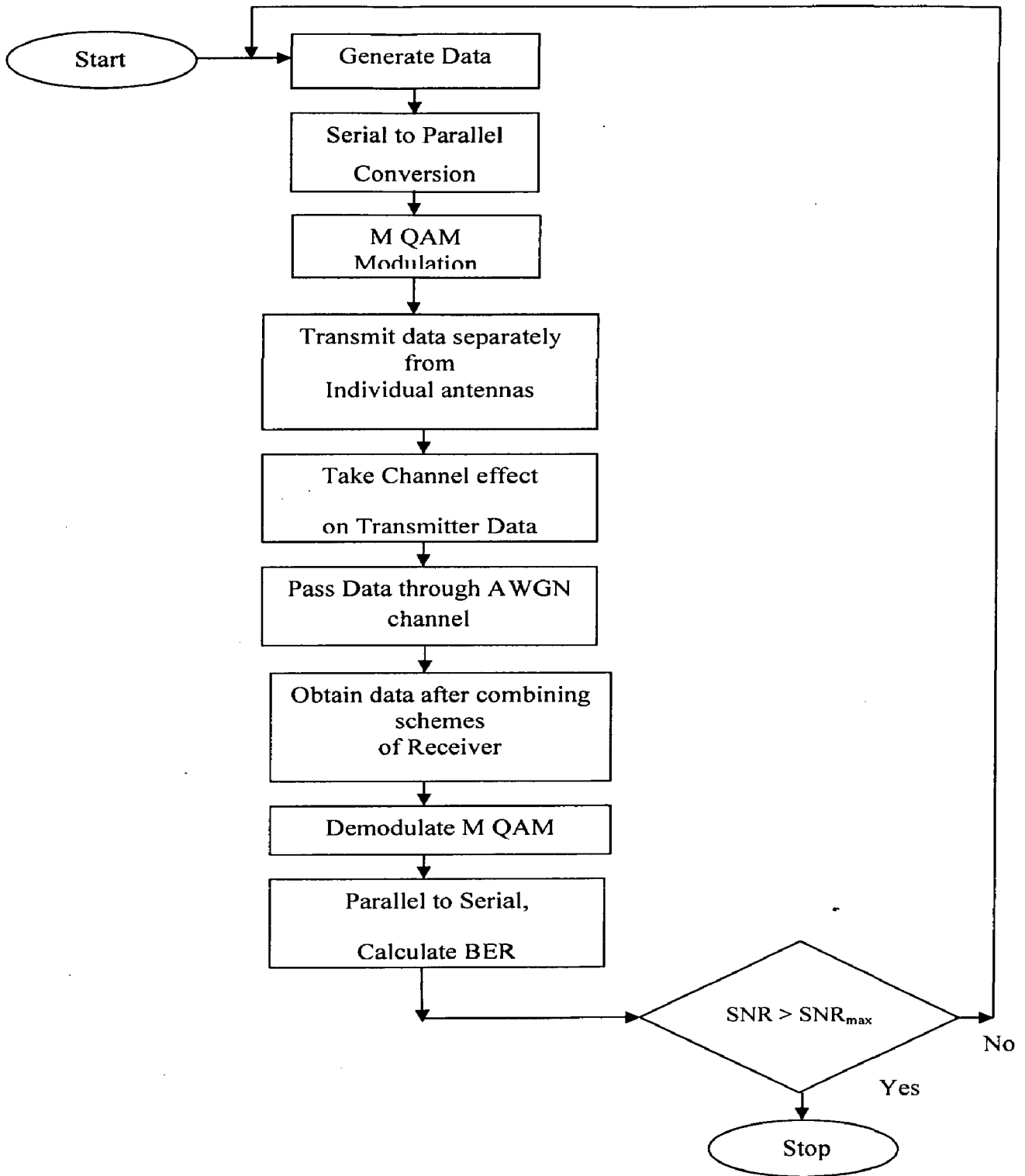


Figure 5.1 Flow chart for implementing Space Time Codes

### 5.3 Flowchart for OFDM

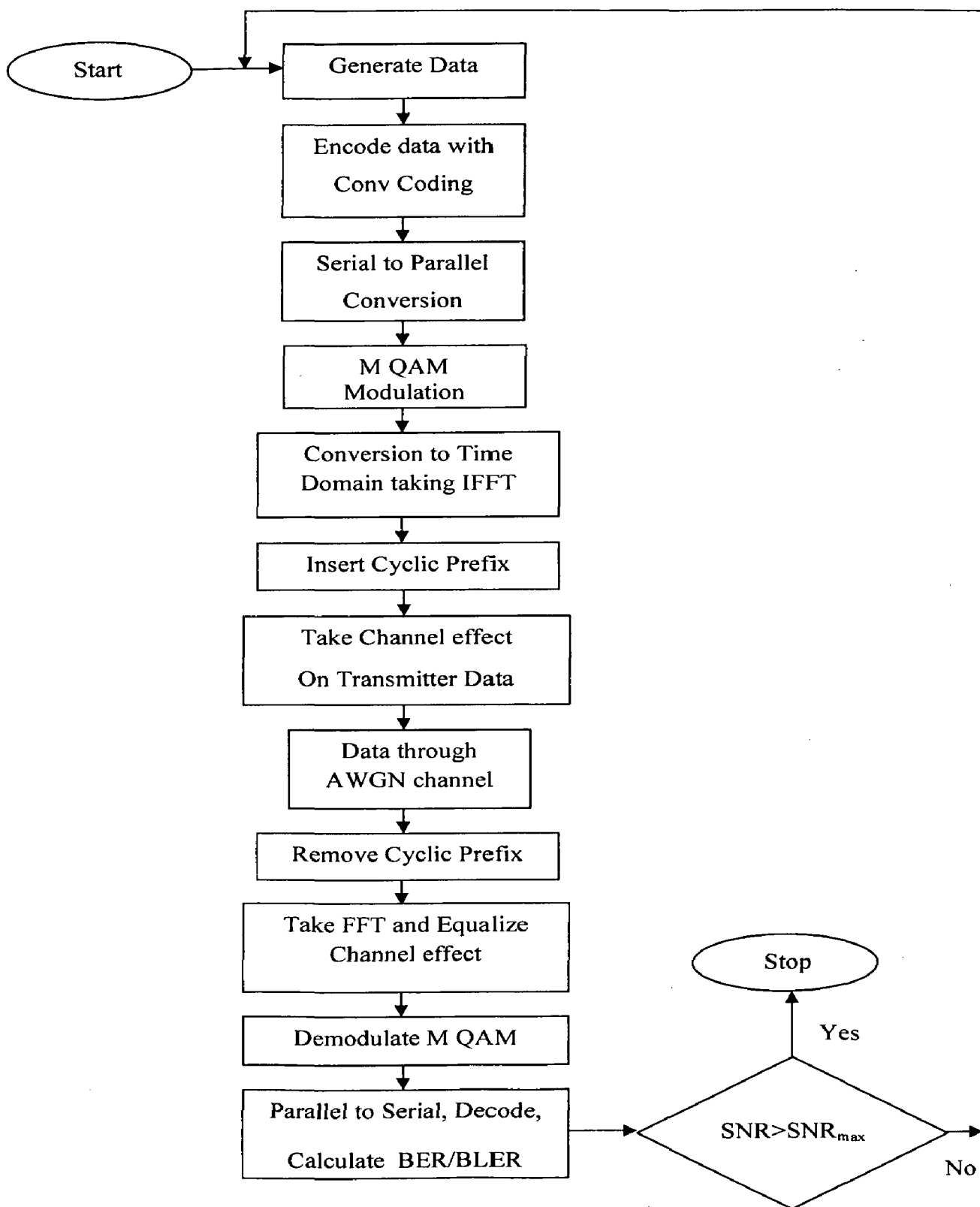


Figure 5.2 Flowchart for implementing OFDM system

### 5.4 Flow Chart used for Simulation of EESM Scheme

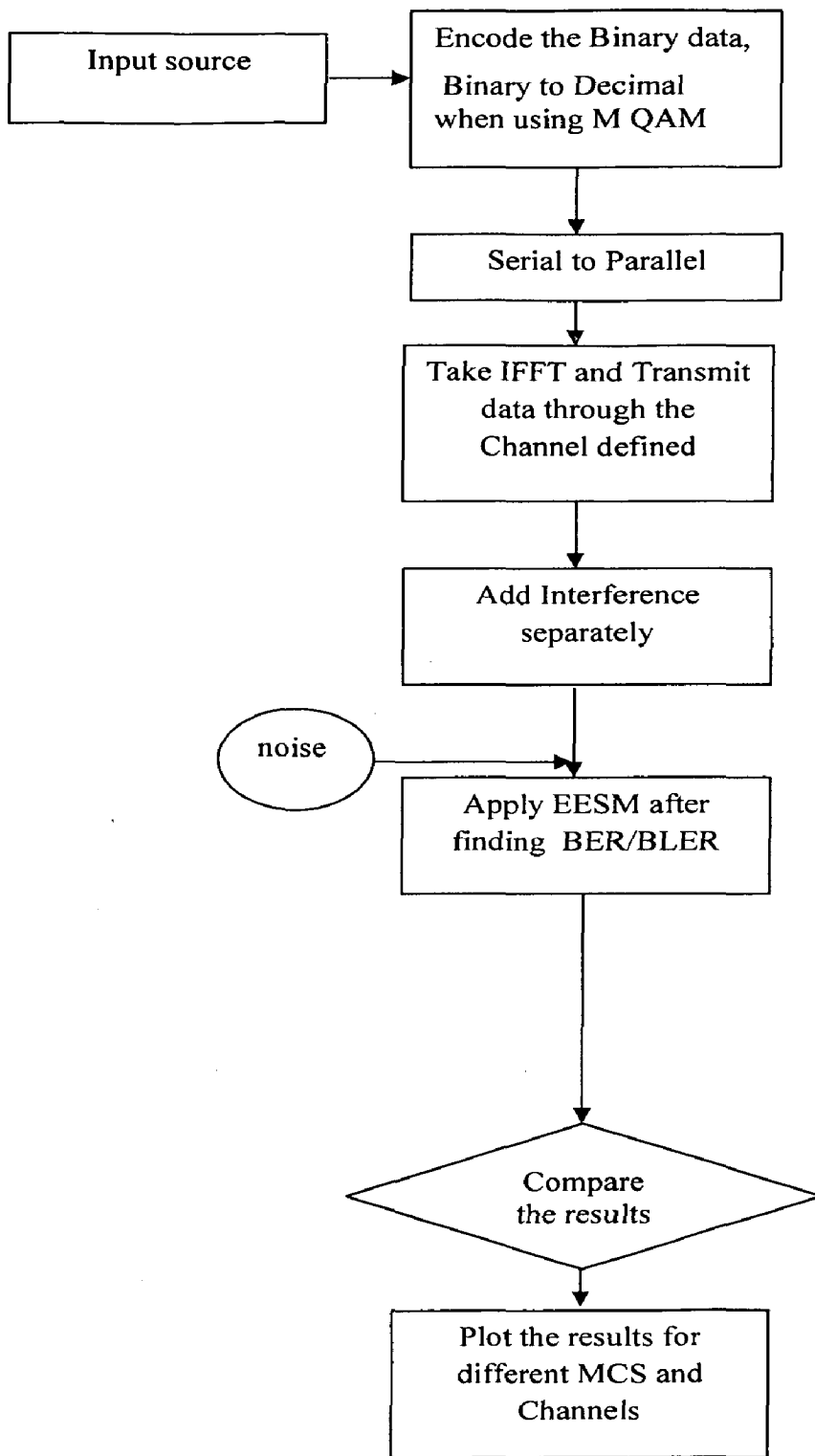


Figure 5.3: Flow Chart used for Simulation of EESM Scheme

## STEPS CONSIDERED FOR SIMULATION

### **iversity advantage through MIMO:**

iversity advantage obtained through implementing the MIMO configuration in the transmission of data is shown in Figure 5.4. Performance is evaluated for while considering a wide range of interest (15/BER). Averaging has been done generating Rayleigh channel in simulations.

Random binary data is directly transmitted after modulation in a SISO case and MIMO cases. When considering Alamouti schemes data is copied to each transmitter and the transmitted sequence at a transmitter is decided by the combining scheme given by Alamouti. In a two Transmitting antenna case, the transmitted power is halved and equally shared for each symbol. The channel is generated every time using two `randn()` functions independently. This information is available at the receiver. AWGN is added to transmitted signal for given SNR. Combining schemes for respective antenna combinations are given in Equations 3.9 and 3.12). A 4 by 2 case is implemented by the implementation of two Alamouti schemes, where 2 more data symbols are considered per block. An independent channel is generated for a transmitter and receiver combination, after which all are averaged to implement a fading channel. A maximum likelihood decoding is used after obtaining data through the receiver. The implementation is done by considering Euclidian distance between the signal received after combiner and all possible signals in the constellation.

It is to be observed through simulations (Figure 5.4), even though the transmitter power is same with increase in transmitting antennas, the scheme performs better compared to SISO. With increase in total (transmit and receive antennas) system performs still better.

### **Comparison of 'beta' (used in EESM abstraction):**

In EESM scheme implementation, the most important thing in evaluating performance of different MCSs is finding the parameter 'beta', through the following steps. Firstly we want to compare the results calculated through the EESM scheme and that of results obtained through simulation of the frequency selective channel.

only first nearest while considering single frequency reuse, cell radius of 1.4 Km. These values obtained are averaged using EESM formula to an effective SINR.

The parameter 'beta' is to be calculated as follows: with equating the BLER in AWGN curve to that obtained in simulating frequency selective case. We obtain corresponding equivalent SINR on the AWGN curve. This process is done for several realizations considering various values. Now select the 'beta' that has the minimum mean square error between the values of SINR obtained through simulations and those calculated through EESM formula. So a value of 'beta' is set for a particular MCS and a particular channel.

#### **Abstraction for EESM:**

After obtaining the 'beta' the implementation of EESM is done for various cases of MCS parameters. Figure 5.5 represents the case of 4 QAM with the case of .5 convolutional code rate. The red line represents the reference AWGN curve calculated for same MCS parameters i.e 4 QAM, .5 coding. No puncturing is done for this case, and hence the data rate remains unaffected. SNR ranges considered are .5 to 1.5 dB for AWGN case. A total of 5,000 blocks are considered for EESM abstraction. A beta value of 1.6 is obtained for this case. The abstractions using EESM formula are shown in green lines. They have been plotted after taking average to effective SINR over each block of data.

A higher data rate is obtained in this case with the punctured coding of the data to be transmitted. The punctured rate of 3/4 is obtained in this case. The Puncturing Matrix  $P = \begin{bmatrix} 1 & 1 & 0 \\ 1 & 0 & 1 \end{bmatrix}$  transmits the upper part of the output sequence as it is and since the binary multiplication of both ones puts it same. For the lower out sequences alternative symbols are dropped for transmission, making the 1/3 code rate to 3/4. For this case also, 5000 blocks of data is sent considering same block size as in previous case. A total of 10 realizations are considered for which obtained results are plotted in Figure 5.6. A loss of nearly 5 dB occurs for this particular scheme for a probability of error of .1 or above. The 'beta' value obtained for this case is 1.7.

The MCS are considered such that the 'beta' parameter gets increased in higher order modulation scheme or higher coding rate. Here the 16 QAM is considered, where the serial to

## 5.5 Results of Simulations

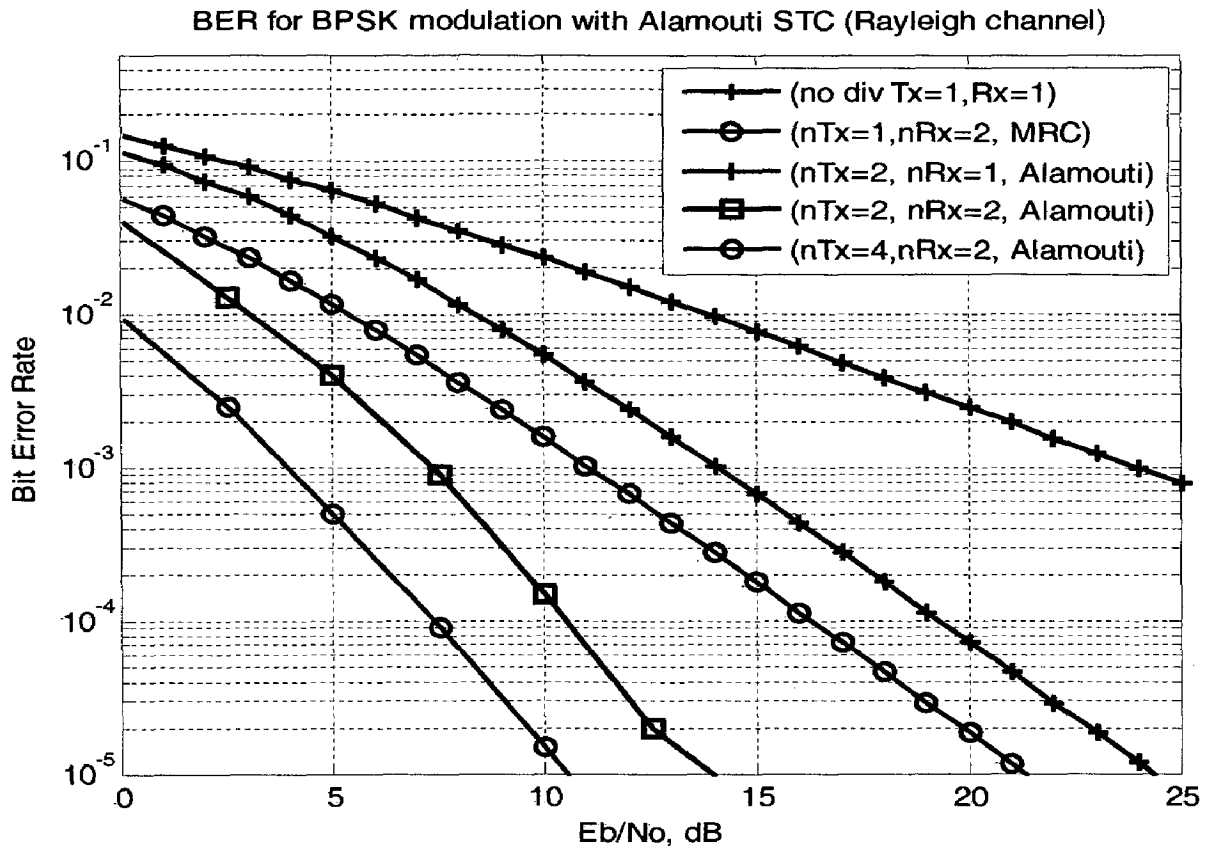


Figure 5.4: BER vs SNR in incorporating Diversity to the Transmission

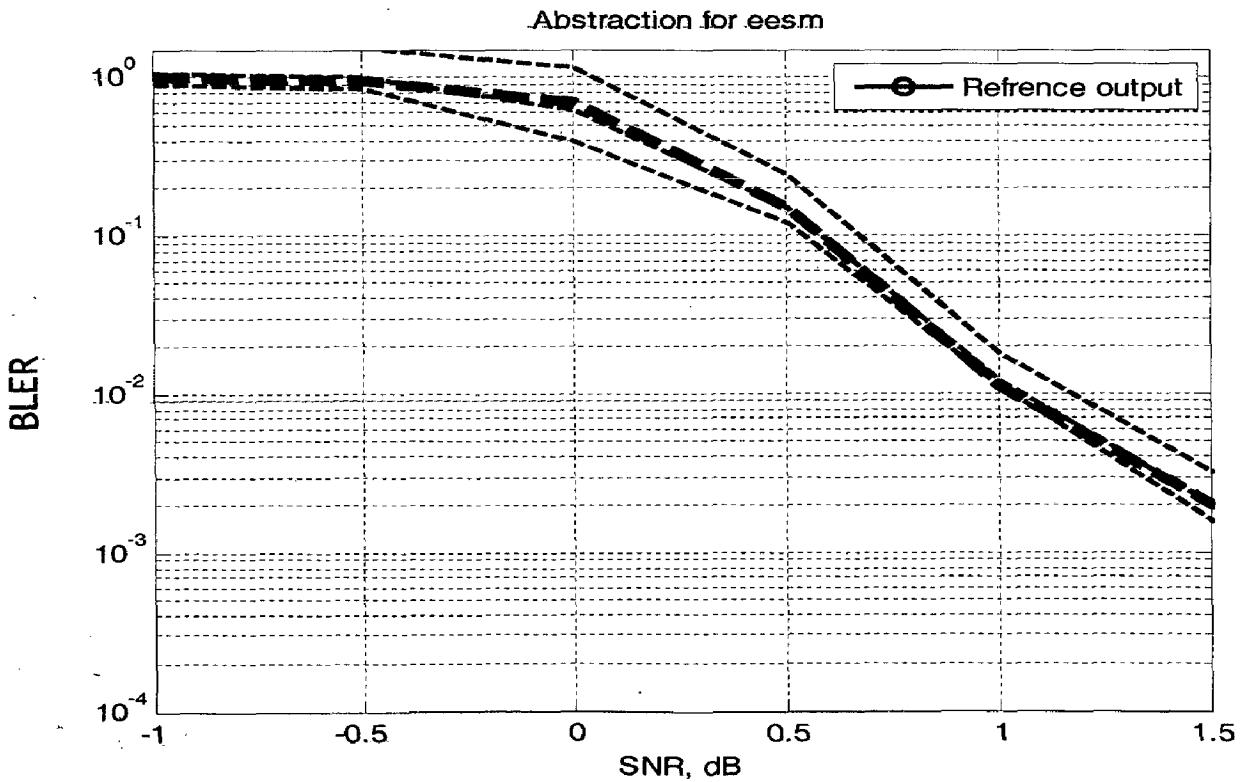


Figure 5.5: EESM Abstraction 4QAM Rate .5 Beta 1.6.



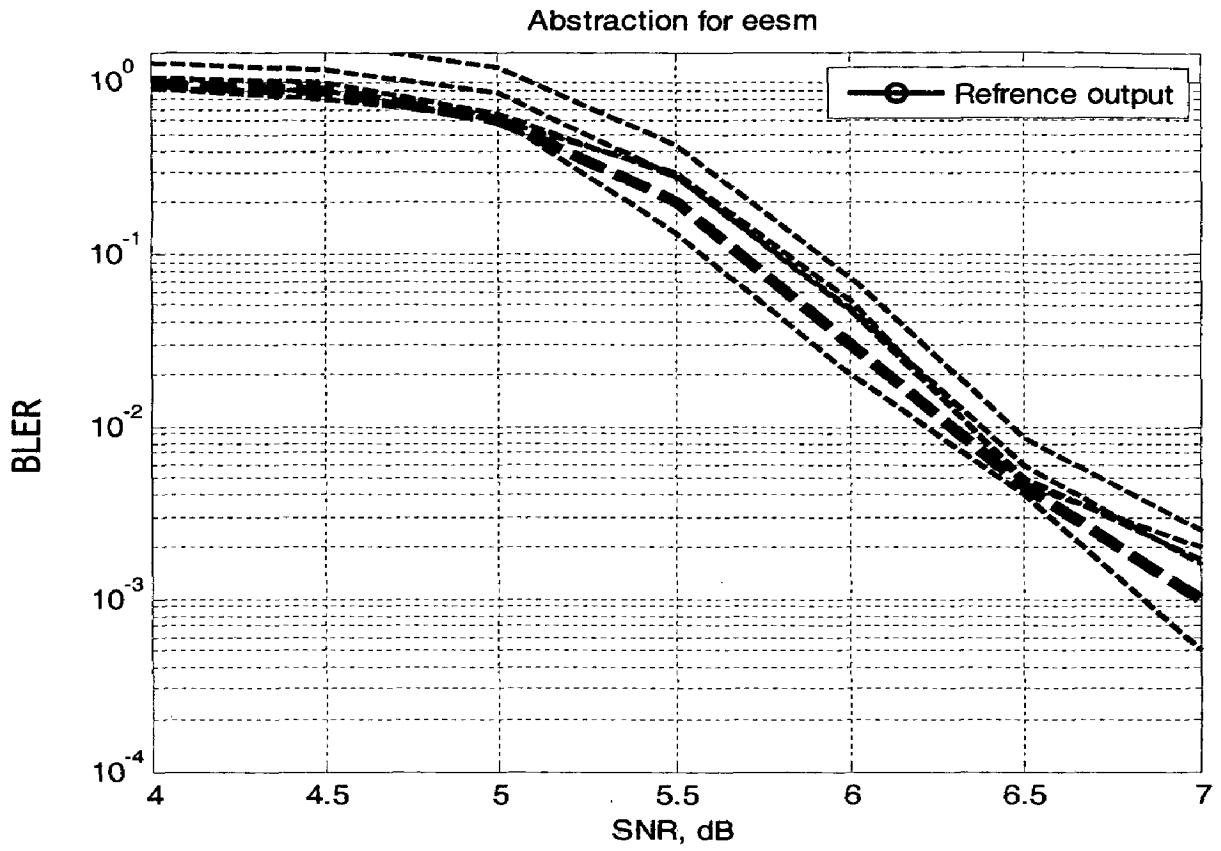


Figure 5.6: EESM Abstraction 4QAM Rate.75 Beta 1.7.

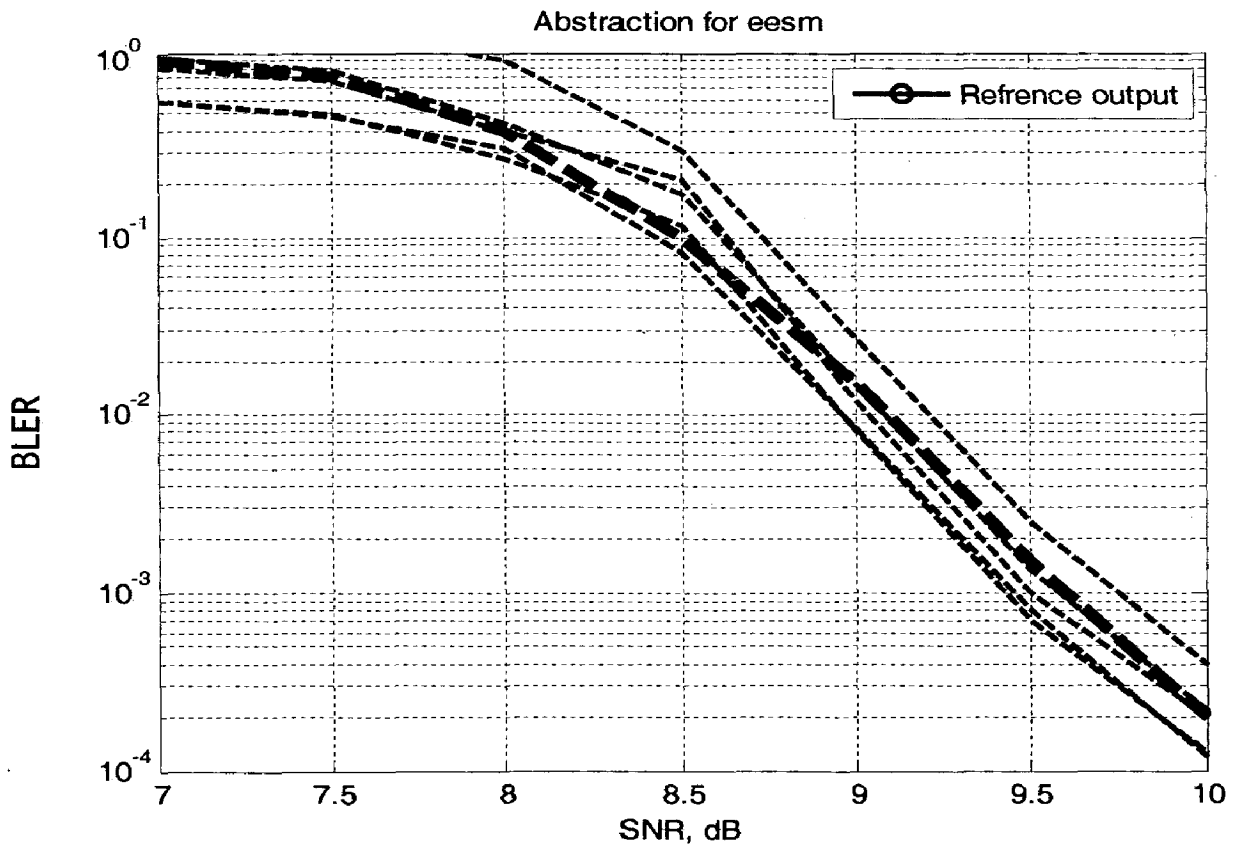


Figure 5.7: EESM Abstraction 16 QAM Rate.5 Beta 5.5

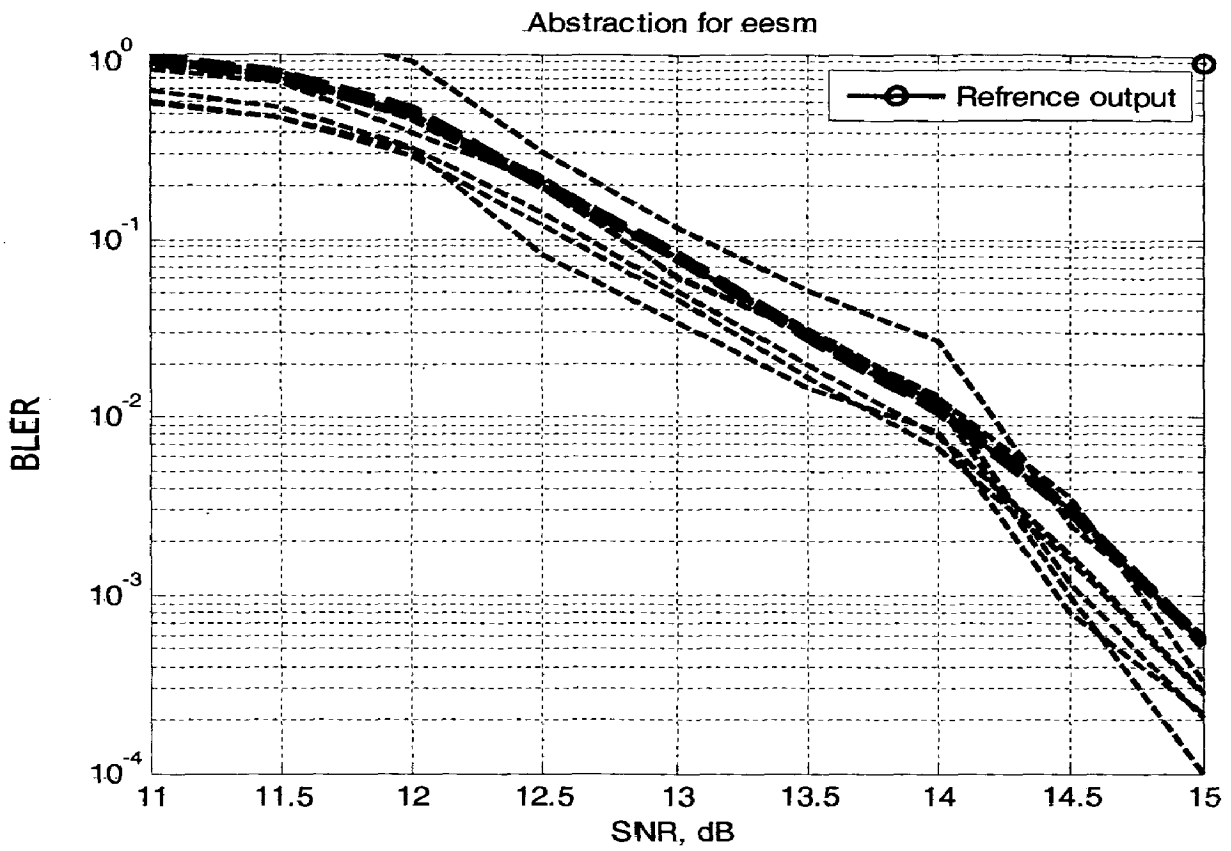


Figure 5.8: EESM Abstraction 64 QAM4 Rate.5 Beta 17.3.

# Chapter 6

## Conclusion

---

WiMAX is considered a strong competitor to the current broadband solutions. Though it is relatively a new technology, many believe that WiMAX will be the next big thing in the wireless communications.

EESM scheme acts as a mediator between Link level and System level Simulations. The relationship between BLER and SINR is mainly dependent on the modulation and coding level used for transmitting data and is also affected by the channel characteristics. In this thesis the BLER vs. SNR graphs to get the desired  $\beta$  values for each common MCS level supported in WiMAX standard have been obtained.  $\beta$  calibration process that requires intensive calculations and simulation steps is still continuing.

When considering in imparting diversity to the transmission, even though restricting the total transmission power with increasing transmitting-receive antennas shows significant improvement in BER.

It is to be observed that the EESM scheme is more accurate for lower order modulation schemes, as compared to higher order modulation schemes.

When considering in imparting diversity to the transmission, even though restricting the total transmission power with increasing transmitting-receive antennas shows significant improvement in BER.

In all Simulations, perfect channel estimation is considered at the receiver. Also perfect synchronization in case of OFDM symbols.

In the future, EESM can be further enhanced by applying Alamouti diversity scheme for transmission.

## References

---

- [1] Niyato and D.Hossain, "WIRELESS BROADBAND ACCESS: WIMAX AND BEYOND-Integration of WiMAX and WiFi: Optimal Pricing for Bandwidth Sharing", IEEE Communications Magazine, vol 24, no 5, pp. 144-148, Sept 2007.
- [2] International Telecommunication Union indicators update-2007.  
[www.itu.int/ITU-D/ict/statistics](http://www.itu.int/ITU-D/ict/statistics).
- [3] Instat Report, [ww.instat.com/press.asp?ID=1634&sku=IN0603199MBS](http://ww.instat.com/press.asp?ID=1634&sku=IN0603199MBS).
- [4] Jeffery G. Andrews, Arunabha Gosh and Rias Muhamed, "Fundamentals of WiMAX", Prentice Hall, ISBN: 0132225522, 2007.
- [5] Steven J. Vaughan-Nichols, "Mobile WiMAX: The Next Wireless Battle Ground", IEEE Transactions on Computer Society, vol.41, no.6, pp. 16-18, June 2008.
- [6] Kejie Lu, Yi Qian, Hsiao-Hwa Chen and Shengli Fu, "WiMAX Networks: From Access to Service Platform", IEEE Transactions on Networks, vol.22, no.3, pp. 38 - 45, May-June 2008.
- [7] P. Robertson and S. Kaiser, "Analysis of the Loss of Orthogonality Through Doppler Spread in OFDM Systems", IEEE Global Telecommunications Conference, vol.1, pp.701-706, Dec. 1999.
- [8] M. Morelli and U. Mengali, "A Comparison of Pilot-aided Channel Estimation Methods for OFDM systems", IEEE Transactions on Signal Processing, vol.49, no.12, pp.3065-3073, Dec. 2001.
- [9] G. Foschini and M. Gans, "On limits of Wireless Communications in a Fading Environment using Multiple Antennas", Wireless Communication Magazine, vol.6, pp. 311-335, Mar. 1998.
- [10] S. Alamouti, "A simple Transmit Diversity Scheme for Wireless Communications", IEEE Journal on Select Areas in Communications, vol.16, no.8, pp.1451-1458, Oct. 1998.

- [11] A. Paulraj, R. Nabar and D. Gore. "Introduction to Space-Time Wireless Communication", 2<sup>nd</sup> Edition, Cambridge University Press, 2005.
- [12] Robert H. Morelos Zaragoza, "The Art of Error Correcting Coding", 2<sup>nd</sup> Edition, John Wiley, 2006.
- [13] S. Nanda and K. M. Rege, "Frame Error Rates for Convolutional Codes on Fading Channels and the Concept of Effective  $E_b/N_0$ ", IEEE Transactions. Vehicular Technology, vol.47, no.4, pp.1245-1250, Nov. 1998.
- [14] S. Lin and D. J. Costello, "Error Control Coding: Fundamentals and Applications", 2<sup>nd</sup> Edition, Prentice Hall, 2005.
- [15] Document from WiMAX Forum, "WiMAX System Evaluation Methodology", Version 2.1, July 7, 2008 <http://www.WiMAXforum.org>.
- [16] C. Ball, "Performance Evaluation of IEEE802.16 WiMAX with fixed and mobile Subscribers in tight reuse", European Transactions on Telecommunications, vol.17, no.2, pp. 203–218, 2006.
- [17] Theodore S. Rappaport, "Wireless Communications Principles and Practice", 2<sup>nd</sup> Edition, Prentice Hall, 2005.
- [18] "System-level Evaluation of OFDM – further considerations", Ericsson, 3GPP TSG- RAN WG1 #35, R1031303, 2003.
- [19] J. G. Proakis, "Digital Communications", 4<sup>th</sup> Edition, McGraw Hill, 2000.
- [20] S. P. Alex and L. Jalloul, "Performance Evaluation of MIMO in IEEE 802.16e/WiMAX", IEEE Transactions on Signal Processing, vol.2, no.2, pp.181-190, April. 2008.
- [21] Nortel Networks, "Effective SIR Computation for OFDM System-Level Simulations", 3GPP TSG RAN WG1 Meeting 35, R1-031370, Lisboa, Portugal, Nov. 2003.
- [22] S. Simoens, S. Rouquette-Léveil, P. Sartori, Y. Blankenship and B. Classon, "Error prediction for Adaptive Modulation and Coding in Multiple-Antenna OFDM Systems", IEEE document, vol. ~~IEEE~~<sup>2</sup>, no. 802.11-03/940r4, May 2004.

[23] Shahid Mumtaz, Atilio Gamberio and Jonathan Rodriguez, "EESM FOR IEEE 802.16e: WiMaX", Seventh IEEE/ACIS International Conference on Computer and Information Science, pp-361-366, May 2008.